THE INFLUENCE OF POROSITY AND CONTACT ANGLE ON INCIPIENT AND DESINENT CAVITATION

Surender Kumar Gupta

Pennsylvania State University
University Park, Pennsylvania

15 December 1969

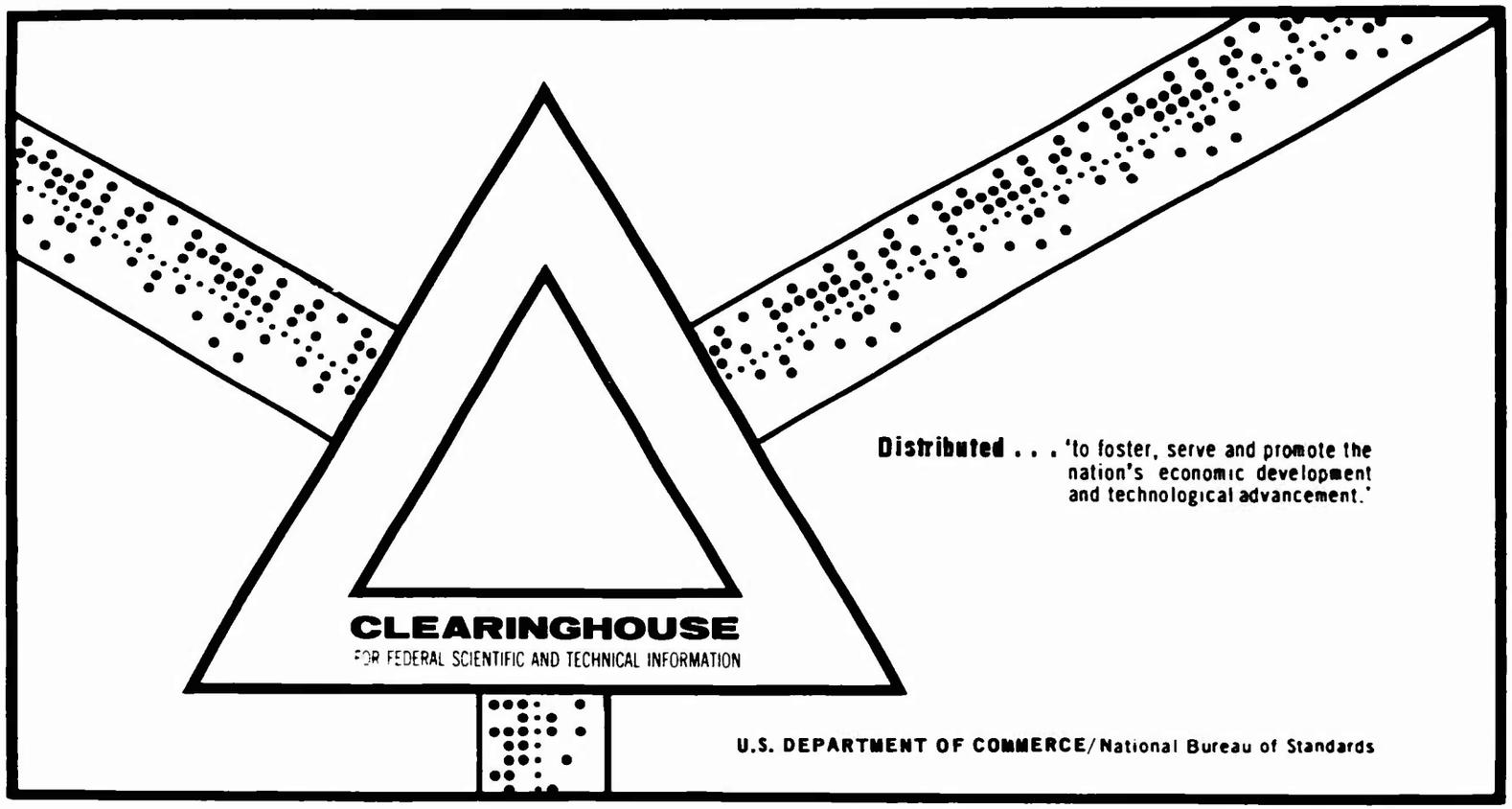

THE INFLUENCE OF POROSITY AND CONTACT ANGLE ON INCIPIENT AND DESINENT CAVITATION

By S. K. Gupta

Technical Memorandum
File No. TM 508.2451-06
December 15, 1969
Contract NOw 65-0123-d
Copy No. 20

The Pennsylvania State University
Institute for Science and Engineering
ORDNANCE RESEARCH LABORATORY
University Park, Pennsylvania

NAVY DEPARTMENT · NAVAL ORDNANCE SYSTEMS COMMAND

File No. 508.2451
December 15, 1969
MS:mac

The Influence of Porosity and Contact Angle on Incipient and Desinent Cavitation

by

Surender Kumar Gupta

ABSTRACT

This investigation was primarily devoted to the determination of the effect of porosity and contact angle on incipient and desinent cavitation. The primary test models were 1/4-inch diameter hemispherical-nosed bodies made of teflon, rubber, polyethylene, stainless steel and glass. The test results imply that the hydrophobic surfaces, i.e., teflon and polyethylene models contribute surface nuclei to the inception process provided that the surface nuclei are in a normal condition, i.e., no effort has been made to minimize surface nuclei by extreme pressurization, etc. On the other hand, the hydrophilic hemispherical models made of glass and stainless steel seem to show no contribution of surface nuclei to the onset of cavitation and may depend entirely on the stream nuclei for cavitation. However, the rubber model which was hydrophilic in nature was not consistent with the other hydrophilic models.

ACKNOWLEDGMENTS

The author expresses his sincere appreciation for the general guidance and useful suggestions during this study by his advisor, Dr. J. William Holl, Professor of Aerospace Engineering.

The investigation was conducted at the six-inch Water Tunnel of the Department of Aerospace Engineering at The Pennsylvania State University under contract with the Naval Ordnance Systems Command.

Appreciation is also expressed to many staff members of the Ordnance Research Laboratory at The Pennsylvania State University whose valuable assistance has contributed a great deal to the successful completion of this study. The readily available help of Mr. R. Husted of the workshop of the Department of Aerospace Engineering is thankfully acknowledged.

The author wishes to acknowledge with thanks the assistance of Dr. P. L. Walker, Jr. and Dr. S. P. Nandi for the porosity measurements of test materials and Mr. B. K. Parekh for the measurements of contact angle.

Thanks are due to Mr. K. N. Swamy for reading the rough draft and offering valuable suggestions.

TABLE OF CONTENTS

TABLE OF CONTENTS (Cont.)

TABLE OF CONTENTS (Cont.)

LIST OF TABLES

LIST OF FIGURES

LIST OF FIGURES (Cont.)

NOMENCLATURE

A, B, C	Names of test series
C_i	Initial gas concentration of the liquid
C_p	Pressure coefficient
$C_{p_{min}}$	Minimum pressure coefficient
D	Diffusivity constant
f	Relative saturation
G1	1/4" glass hemispherical-nosed model #1
N_s	A constant for determining the surface area of a liquid-gas interface
N_v	A constant for determining the volume within a surface nucleus
P	Porosity, Equation (A.5), cc/cc
P1	1/4" polyethylene hemispherical-nosed model #1
P_∞	Free stream static pressure in the test section, psia
P_{∞_d}	Free stream static pressure in the test section corresponding to desinence of cavitation, psia
P_{∞_i}	Free stream static pressure in the test section corresponding to the inception of cavitation, psia
P_L	Liquid pressure, psia
P_{min}	Pressure at the minimum pressure point of the model, psia
P_{min_i}	Pressure at the minimum pressure point of the model at inception, psia
P_v	Vapor pressure for inception runs, psia

P_v	Vapor pressure, psia
R	Radius of the liquid-gas interface at time t, inches
R1	1/4" rubber hemispherical-nosed model #1
RO1	1/4" rubber zero caliber ogive model #1
R_o	Radius of the liquid-gas interface at time t equal to zero, inches
R_f	Final radius of the liquid-gas interface, inches
R_s	Specific gas content
r	Bubble radius at desinence, Equation (5.2), inches
S	A parameter for wetting phenomenon, Equation (2.4)
S1	1/4" stainless steel hemispherical-nosed model #1
T	Liquid temperature Equation (5.9), ^oR
T1	1/4" teflon hemispherical-nosed model #1
TO1	1/4" teflon zero caliber ogive model #1
T2	1/4" teflon hemispherical-nosed model #2
t	Growth time for the liquid-gas interface, seconds
t_{cal}	Calibration time, seconds
t_d	Delay time for incipient cavitation, seconds
t_i	Inception time, seconds
V_∞	Free stream velocity in the test section, fps
x	Non-dimensional growth time for the liquid-gas interface
α	Total air content of liquid, ppm
α_d	Dissolved air content of liquid, ppm
α'	Angle of attack, degrees
β	Henry's Law constant

γ	Surface tension of liquid, lb_f/in
γ_{LG}	Free energy at the liquid-gas interface
γ_{SG}	Free energy at the solid-gas interface
γ_{SL}	Free energy at the solid-liquid interface
δ	A parameter, Equation (5.7)
ϵ	Ratio of liquid-gas interface radius at time t to liquid-gas interface radius at t equal to zero
θ	Contact angle, degrees
θ'	Pore volume of a material per unit mass, cc/gm
ρ_{He}	Helium density of a material, gm/cc
ρ_{Hg}	Mercury density of a material, gm/cc
ρ_L	Liquid density, $lb_f\text{-}sec^2/in^4$
σ	Cavitation number
σ_d	Desinent cavitation number
σ_i	Incipient cavitation number
Φ	Half angle of a conical surface cavity, Figure 20, degrees

UNITS

fps	Feet per second
in	Inches
lb	Pounds
lb_f	Pounds force
ppm	Parts of air per million parts of liquid
psi	Pounds per square inch
psia	Pounds per square inch absolute

sec	Second (a measure of time)
cc/cc	Cubic centimeter per cubic centimeter
gm/cc	Grams of mass per cubic centimeter
^{o}R	Degrees Rankine (a measure of absolute temperature)

CHAPTER I

INTRODUCTION

1.1 Motivation for the Investigation

It is well known in the operation of liquid handling machinery that vapor- and gas-filled voids are often created by dynamic action in the liquid so that the flow is no longer single phase. The occurrence of these vapor- and gas-filled voids in the otherwise liquid flow is called cavitation.

Cavitation may be characterized by the growth and collapse of many bubbles. This creates noise and, under some circumstances, may lead to the erosion of the boundary surfaces due to the very high local pressure associated with collapsing bubbles. Thus, cavitation in all of its forms is of great practical interest and has been studied for many years.

In a liquid system, cavitation can be initiated by lowering the pressure or, once started, it can be eliminated by increasing the pressure. The former is called incipient cavitation, whereas the latter is referred to as desinent cavitation. These two types of cavitation were the major concern in this investigation.

1.2 Previous Investigations

Incipient cavitation was studied by Eurich (7)* who conducted some tests with hemispherical-nosed models on a rotating arm in a cavitation tank. From his experiments, he concluded that a decrease in the total air content caused an increase in delay time, whereas the trend of decreasing delay time was associated with increasing velocity.

The conclusions of Eurich's study were further strengthened by Treaster (20) when he performed a series of tests with the 1/4" stainless steel model with a hemispherical nose. Though it was generally felt by Treaster that free-stream nuclei might be the primary source of cavitation, his tests with teflon implied a contribution from the surface. He observed very short delay times with teflon and suggested that these might be attributable to the porous and hydrophobic nature of the material. Also he observed an effect of exposure pressure on delay time.

An extensive study of the effects of surface characteristics on the inception of cavitation was carried out by Reed (18). He took various models made of materials having different combinations of porosity and contact angle for his tests and found that porosity plays an important role in the onset of cavitation. He showed that teflon, which has a hydrophobic and porous surface, has a very small delay time whereas glass, which has a non-porous and hydrophilic surface, may have a long delay time.

---

* Numbers in parentheses indicate the reference number

Another important conclusion drawn from Reed's investigation indicated that the pressure history has an important influence on the inception of cavitation. This means that a pressurization of the liquid-model system prior to a test would tend to increase the delay time whereas an exposure to continued low pressure would be conducive to rapid inception of cavitation. The only exception to this observation was the solid teflon nose which was not influenced by pressure history.

Reed also introduced a theory to explain the cavitation delay time. However, the theoretical results did not appear to explain the experiments. Furthermore, some of Reed's conclusions were of a tentative nature because it was not always possible to separate the effects of surface nuclei from those due to stream nuclei.

1.3 Statement of the Problem

The major objective of this investigation was to determine the influence of surface characteristics on incipient and desinent cavitation. The surface characteristics of concern were porosity and contact angle, and special procedures were employed to separate the effects of stream and surface nuclei.

1.4 General Scope of the Investigation

Incipient and desinent cavitation, both vaporous and gaseous were investigated. The cavitation experiments were conducted in the Water Tunnel of the Department of Aerospace Engineering at The Pennsylvania State University. The Water Tunnel is shown in Figures

1 and 2. The internal diameter of the circular test section was six inches. For this tunnel, two test section velocities were possible, namely, 29 fps and 39 fps. The higher velocity was used in most instances during this investigation.

Tests were conducted at two extreme values of total gas content, namely, 5 and 18 ppm (the quantity ppm meaning parts per million is equal to the number of moles of air per million moles of water). These extreme values were employed in order to produce a large variation in both dissolved and free gas content.

The models employed in this investigation and shown in Figure 3 were bodies of revolution with a cylindrical afterbody and had a hemispherical (0.5 caliber ogive) or zero caliber ogive nose. All models were 1/4" in maximum diameter. The hemispherical noses were made of glass, stainless steel, rubber, polyethylene and teflon. Some of these models had been used previously by Treaster (20), Holl and Treaster (14), and Reed (18). Most of these tests were conducted with the hemispherical noses, but a limited number of tests were conducted with zero caliber ogives made of teflon and rubber.

In addition to the aforementioned cavitation experiments, the models were tested in a tank under non-flow conditions in order to observe bubble evolution on the surface.

CHAPTER II

FUNDAMENTALS

2.1 Basic Definitions

In this section, we define a few of the basic terms which are frequently employed in this thesis.

(a) Vapor and Gas. It is important to distinguish between the various gas phases which may be present in the cavitating flow. The word vapor refers to the gas phase of the liquid, whereas the word gas will refer to the noncondensable gas such as air in water. A gas is a permanent state of matter which cannot be converted to liquid or solid state easily.

(b) Contact Angle (θ). Contact angle is defined as the angle measured between the tangents drawn to the liquid surface and solid surface at the point of contact and measured through the liquid phase. Thus, for a surface, it is to some extent a measure of the wettability by water. The surfaces which are wetted by water are called hydrophilic, while those which shed water are known as hydrophobic. Glass which is wetted by water has a very small contact angle, whereas teflon, which sheds water, has a large contact angle.

(c) Porosity. Porosity is a measure of the void space in any material and is defined as.

$$P = \frac{\text{Volume of the void space}}{\text{Total volume of the material}} .$$

Thus, a more porous material will have a larger amount of gas trapped in its void space than does a less porous material.

(d) Delay Time. Delay time is defined as the time lag for incipient cavitation. It is measured from the time when the inception pressure is established to the time when cavitation first appears. Delay time has been employed by several investigators (7,14,18,20).

(e) Inception Time. A new quantity which was found to be useful during this study is the inception time. This time is measured from the time the water tunnel is started to the time when cavitation first appears. Thus, it should be noted that the flow is unsteady during the whole or part of the inception time.

2.2 Wetting Phenomenon

The value of the contact angle is not always a reliable measure of molecular attraction between the solid and the liquid. Contact angle depends on all three phases in contact and can give information only on the relative strength of the attractions between solid and liquid on one hand and solid and gas on the other hand; the greater the first attraction compared with the second, the smaller the contact angle. However, the solid-liquid attraction can still be very strong even if the contact angle is large (3).

As seen from Figure 4, the equilibrium equation for contact angle is:

$$\gamma_{SG} - \gamma_{SL} = \gamma_{LG} \cos \theta \, . \tag{2.1}$$

Thus, the wetting of a solid substance by a liquid depends not only on contact angle, but on three additional quantities, namely, γ_{SG}, γ_{SL}, and γ_{LG}. Cooper and Nuttall (5) first defined the condition for wetting of a substance by a liquid. The condition for wetting is:

$$S > 0 \, , \tag{2.2}$$

and for nonwetting:

$$S \leq 0 \, , \tag{2.3}$$

where

$$S = \gamma_{SG} - (\gamma_{SL} + \gamma_{LG}) \, . \tag{2.4}$$

Free energy or surface tension depends not only on the constituents of the solid material, but also on the impurities in the liquid. Thus, wettability is a function of all three phases in contact (10).

2.3 Flow Regimes

There are three main regimes of flow for the investigation of cavitation. These regimes are characterized by the amount of cavitation present in the flow.

(a) Non-Cavitation. As the name suggests, this condition refers to a flow situation of only one liquid phase. No cavitation bubbles are created in the flow. This usually occurs at relatively high liquid pressures and can be clearly observed and distinguished.

(b) Developed Cavitation. This regime is reached at very low pressures where most of the surface is under cavitation. It is a state of vigorous cavitation and is easily observed.

(c) Limited Cavitation. Limited cavitation occurs at pressures between those for non-cavitation and developed cavitation. As the name implies, the number of cavitation bubbles present for limited cavitation is small.

In some cases, for this flow regime, the cavitation may not be continuous over the surface nor with respect to time. This means that there may be only a few spots of cavitation on the surface and that the cavitation may appear and disappear in a random manner.

2.4 Types of Cavitation

In this section, the emphasis is on the different mechanisms by which cavitation may take place.

(a) Vaporous Cavitation. When the pressure in any region of the flow falls below the vapor pressure of the liquid, small gas bubbles in the surface and/or liquid may suddenly grow explosively without bound. The growth is essentially caused by the rapid conversion of liquid to vapor and is called vaporous cavitation.

(b) Gaseous Cavitation. For gaseous cavitation, bubbles which may already be present in the liquid grow through the transport of gas. The main factor affecting this type of cavitation is clearly the gas concentration of the surrounding liquid. If the liquid is undersaturated, no gaseous cavitation will occur; whereas if the liquid is over saturated, this type of cavitation will readily occur.

(c) Pseudo Cavitation. When a gas bubble merely responds to a change in liquid pressure by changing the size, pseudo cavitation occurs. Thus, in pseudo cavitation, no transfer of mass takes place.

(d) Desinent and Incipient Cavitation. Two additional types of cavitating flows are those of desinence and inception. If the velocity is held constant and cavitation established, then desinent cavitation can be attained by slowly increasing the pressure until all cavitation disappears. On the other hand, incipient cavitation is attained if all cavitation is first eliminated and the pressure lowered so that cavitation finally appears at constant velocity.

2.5 Cavitation Number

In aerodynamics, one of the most fundamental and useful quantities for understanding the performance of an airfoil is the dimensionless pressure coefficient. Of particular concern in cavitation is the minimum pressure coefficient given by:

$$C_{Pmin} = \frac{P_\infty - P_{min}}{1/2\ \rho_L\ V_\infty^2} \quad . \tag{2.5}$$

To have a clearer understanding of the cavitation phenomenon, we employ the cavitation number, σ, given by:

$$\sigma = \frac{P_\infty - P_v}{1/2\ \rho_L\ V_\infty^2} \quad , \tag{2.6}$$

where P_v is the vapor pressure corresponding to the bulk temperature of the liquid.

Therefore, corresponding to the states of incipient and desinent cavitation, we have the two cavitation numbers:

$$\sigma_i = \frac{P_{\infty_i} - P_v}{1/2\ \rho_L\ V_\infty^2} \quad , \tag{2.7}$$

and

$$\sigma_d = \frac{P_{\infty_d} - P_v}{1/2\ \rho_L\ V_\infty^2} \quad , \tag{2.8}$$

σ_i being called the incipient cavitation number and σ_d the desinent cavitation number.

From the experimental evidence, it appears that in many cases:

$$\sigma_i \leq \sigma_d \quad . \tag{2.9}$$

Also, for vaporous cavitation to take place, it is necessary that:

$$P_{min} \leq P_v \quad . \tag{2.10}$$

This implies that, for vaporous desinent cavitation,

$$\sigma_d \leq C_{Pmin} \quad , \tag{2.11}$$

and hence, in general, we can state that, for vaporous cavitation,

$$\sigma_i \leq \sigma_d \leq C_{Pmin} \quad . \tag{2.12}$$

In some cases, it is also possible to obtain gaseous incipient and desinent cavitation such that,

$$C_{Pmin} < \sigma_i \leq \sigma_d \quad . \tag{2.13}$$

In theory, the condition,

$$\sigma_i = \sigma_d \quad , \tag{2.14}$$

is a possibility, but sometimes in practice it is observed that if we

set σ_i equal to σ_d, we may in some cases have to wait for a significant period of time before any cavitation can be observed. Therefore, for practical purposes, during inception runs, σ_i is usually set at a value lower than σ_d. The difference between σ_d and σ_i is sometimes taken as a measure of cavitation hysteresis (14).

CHAPTER III

GENERAL TESTING PROCEDURES

3.1 Description of Major Equipment

The water tunnel used for this investigation had a plexi-glass test section of circular cross section and six-inch inside diameter. The length of the test section was 24 inches. The diameter of the settling section upstream of the test section was 18 inches giving a contraction ratio of three. Neither honeycombs nor screens were employed in the settling section. A photograph of the Water Tunnel in the region of the test section is shown in Figure 1 and the tunnel circuit is shown in Figure 2.

Two free-stream, test section velocities were possible for this tunnel, namely 39 fps and 29 fps. The velocity was measured with the help of a mercury-water manometer.

To measure the static pressure in the test section, a hole was drilled directly below the model nose in the wall of the test section, and a lead from this hole was connected to a standard Heise gauge which could be calibrated at atmospheric pressure in order to give the value of the absolute pressure directly.

The pressure in the tunnel was controlled with the help of an air column in the stand pipe (refer to Figures 1 and 2). By increasing the pressure of air in the stand pipe to about 75 psi, an absolute pressure of about 85 psia was obtained in the test section, whereas a low pressure of about 10 psia was obtained, in non-flow conditions, by reducing the air pressure to atmospheric value. The pressure control valves are shown to the right of Figure 1.

In order to measure the total air content of the tunnel water, the standard Van Slyke apparatus was employed. Also, the inception time measurements were carried out with the help of an electronic counter which had remote control on and off switches.

3.2 The Test Models

Eight different models, made of five different materials, were employed during this study. Characteristics of these models are noted in Table 2. The porosity measurements were made by the "Helium-Mercury Density" measurements (9,17) as explained in Appendix A. The contact angle measurements are discussed in Appendix B. Unless otherwise stated, all models had a hemispherical nose. A photograph of the models is shown in Figure 3. The eight models were

(a) 1/4" Glass #1 (Designated G1). The solid glass nose had a stainless steel afterbody. It was the same model as employed by Reed (18).

(b) 1/4" Stainless Steel #1 (Designated S1). This was the same model as employed by Treaster (20) under the designation ORL Hemisphere B, by Holl and Treaster (14) as ORL B, and by Reed (18).

(c) 1/4" Rubber #1 (Designated R1). This model was first made for this investigation and had a rubber nose with a stem of stainless steel.

(d) 1/4" Polyethylene #1 (Designated P1). This model, made for this study, had a stem made of stainless steel.

(e) 1/4" Teflon #1 (Designated T1) This model was employed by Holl and Treaster (14) and Reed (18) and was designated the solid teflon model in their investigations.

(f) 1/4" Teflon #2 (Designated T2). This was an additional teflon nose with stainless steel stem similar to the teflon #1 model and was made for the present investigation

(g) 1/4" Rubber Zero Caliber Ogive #1 (Designated R01) and 1/4" Teflon Zero Caliber Ogive #1 (Designated T01). These models were both made for this study and had stainless steel afterbodies with rubber and teflon noses

3.3 Standard Conditions for Tunnel Testing

In the course of this investigation, all the tests were divided into three main categories, depending upon three nearly standard initial conditions. The three sets of tests are referred to as Series A, B, and C.

3.3.1 Series A. This series was commonly referred to as the maximum-minimum series. This means that, for tests conducted in this series, an attempt was made to nearly maximize the surface nuclei and minimize the stream nuclei.

The procedure employed to obtain the required nuclei situation for the surface was to keep the model in an atmosphere of air for nearly 24 hours at a pressure of about 75 psi. After this, the model was sting-mounted in the test section with a lucite cap, Figure 5, covering the model so that water did not disturb the surface until testing began (refer to Appendix C for additional details).

To minimize the stream nuclei, the air content of the water was kept reasonably low, varying between 4.86 ppm and 6.10 ppm. In addition, the tunnel water was further pressurized to an average of about 70 psia for nearly 20 hours after deaeration. This was done with the understanding that the stream nuclei which are left in the water after deaeration would be further reduced in the highly undersaturated water.

At the beginning of a test in this series, the model was uncapped by pulling the lucite cap off the model with the help of an attached string. During this process, the model surface was exposed to water for about 7 to 10 minutes at atmospheric pressure before the first inception run was conducted.

3.3.2 Series B. This was called the minimum-minimum series. Thus, for this test series, an attempt was made to minimize both types of nuclei.

To reduce the surface nuclei to a minimum, the model was kept in water for about 24 hours at a pressure varying between 200 psi and 1200 psi. These values of high pressure in static water were obtained by using the same high pressure hand pump as employed by Reed (18) and

also by Brown (4). This pump is shown to the left in Figure 1. After pressurizing the model with water, mostly in a static jacket, procedures were employed to prevent exposure of the model to air. For this purpose, the nose was removed from the static jacket or static tank, shown in Figure 6, placed in a water tank and then transferred to the lucite cap filled with water. The model with the cap was then sting-mounted in the test section. After filling the tunnel with water, the cap was removed and deaeration carried out. The model was further pressurized along with the tunnel water to get a condition of minimum stream nuclei as well as to further pressurize the model surface. This pressurization was at the same pressure level as employed in Series A, namely, 70 psia for 20 hours. The total air content for Series B varied from 4.35 ppm to 5.53 ppm.

3.3.3 Series C. The last test series was characterized by the name minimum-maximum. Here an attempt was made to maximize the stream nuclei and minimize the surface nuclei.

The condition of minimum surface nuclei was realized by pressurizing the model in static water in the same manner as was done in Series B. To get an abundance of stream nuclei, the tunnel was completely filled with fresh tap water at the beginning of each test. A total air content of about 15 ppm to 19 ppm was characteristic of this water.

It is important to note that the use of the words "maximum" or "minimum" in the preceding paragraphs with respect to the number of surface or stream nuclei, is open to question. There was no method

available, during this investigation, to actually find the number and size of the nuclei present.

3.4 Standard Tunnel Runs

Only two kinds of standard runs were carried out for each test, these being the inception and desinence runs

3.4.1 Inception Runs. In general, a fixed value of the set pressure was chosen, namely, 15.3 psia. The pressure in the tunnel was set at this value before starting the tunnel for each inception run. After this, the tunnel and the timer were simultaneously started and the model nose observed for the onset of cavitation. The timer was stopped at the first appearance of cavitation at any point or region of the model nose. The time measured from the starting of the tunnel to the first appearance of cavitation was called the inception time (refer to Appendix D and Figures 7 through 11 to obtain the value of P_{∞_i} from the inception time, t_i).

The value of 15.3 psia for a set pressure was selected so that the tunnel attained a steady state pressure of about 5.4 psia. The test section pressure of 5.4 psia was nearly the lower bound for good operational conditions for the particular pump-tunnel combination employed in this investigation. At pressures less than 5.4 psia, a large number of bubbles would be created in the stream. This would prevent the realization of the condition of minimum stream nuclei and also the flow would become unsteady.)

For some inception runs, the model-tunnel system was pressurized to about 85 psia for 10 minutes in most cases and for 15 to 30 minutes in some cases, prior to the inception run, other details being the same as before.

For a small number of tests, some additional inception runs were carried out at higher values of the inception pressure or set pressure. This was done to get some insight into incipient gaseous cavitation.

3.4.2 Desinence Runs. The standard procedure followed for the desinent cavitation runs was much simpler. To start with, a steady flow was first established and then the pressure lowered to about 5 psia to obtain a cavitating flow. Afterwards, the pressure was gradually increased until all cavitation disappeared. The corresponding value of the pressure was noted as the desinent cavitation pressure P_{∞_d}. Most of these runs were carried out at the higher speed of about 39 fps. Only a limited number of runs, for a few tests, were performed at the lower speed of about 29 fps.

CHAPTER IV

VISUAL OBSERVATIONS

4.1 Static Tests

In order to obtain some information about the surface nuclei for the different materials in various conditions, four test series were performed with the stainless steel, rubber polyethylene and teflon models with the help of the static tank and/or static jacket shown in Figure 6. All of the tests with these devices were conducted under essentially static conditions.

For test series #1, the tank was filled with water after a model was mounted in the tank. A vacuum of about 26 inches of mercury was then applied at the top of the tank and the model nose was carefully observed through a microscope for the evolution of bubbles. This was called "the first application of vacuum in water" and is referred to as the reference state. Noting the results for the various surfaces, we find that hydrophobic surfaces such as teflon and polyethylene give rise to a profuse bubbling from the surface. The evolution of bubbles for the reference state of the stainless steel surface was much less than that of the hydrophobic surfaces but still many bubbles were observed. On the other hand, the rubber nose showed an even smaller number of bubbles than that of the stainless steel nose.

For test series #2, the water-model system was pressurized by the hand pump shown to the left in Figure 1 to about 80 psi for a period of about 10 minutes. Then, the pressure was reduced to about 1 psia inside the tank and the nose observed for bubbles. This procedure was repeated two or three times for some models. As a result, a marked difference in the evolution of bubbles was observed. In the case of the stainless steel, only one bubble was observed initially; however, after about 5 to 10 minutes, one more bubble appeared. As the process of applying high water pressure was repeated, the stainless steel surface showed a trend of reduced bubbling. For the rubber nose, no bubble was observed in the beginning but, if the application of vacuum was continued for periods of time greater than forty minutes, one or two bubbles eventually appeared on this nose. In order to investigate further, the rubber nose was first kept in an atmosphere of air at about 75 psi for about 4 hours and was then pressurized at about 80 psi in water for about 10 minutes. When a vacuum of the same level as used before was applied in water, a bubbling approximately equal to that of the reference state was noticed. For the polyethylene nose, only one bubble was observed in test Series #2. On the other hand, the teflon surface gave rise to several bubbles in test Series #2.

A special test was conducted with the teflon #1 nose. The model was kept in water in the static jacket for about 24 hours at a pressure of about 1125 psi. It was then transferred to the static tank without exposing it to air and pressurized for about 22 hours at a water pressure of about 80 psia. In this way, an attempt was made to

simulate the conditions applied to obtain a minimum number of surface nuclei in test Series B and C of the tunnel program. Finally, when the pressure was reduced to about 1 psia, one or two bubbles came out of the surface after about 13 seconds and continued to come out for times to 45 minutes without any additional bubbles appearing.

In test Series #3, the models were subjected to an air atmosphere at 75 psi for about 10 minutes. The purpose of this procedure was to force the models to regain surface nuclei following test Series #2 in which the models tended to lose nuclei as a result of pressurization with water. As a result of applying the high pressure air, it was found that the surfaces appeared to regain some nuclei in all cases but to a varying degree. In a period of 10 minutes, the stainless steel nose appeared to have nearly regained its reference state, whereas the rubber nose did not attain the reference state although it regained a few bubbles. Also, the reference state was not restored for the hydrophobic surfaces. Polyethylene regained only a few bubbles whereas teflon regained many bubbles.

The purpose of test Series #4 was to observe the effect of keeping the models in water for a prolonged period of about 24 hours at atmospheric pressure. It was observed that by this process, the rubber model lost almost all of its surface bubbling, whereas the other substances did retain some surface bubbling but it was very much reduced from that corresponding to the reference state.

No results for the glass nose have been reported in the preceding paragraphs due to the fact that this nose was not employed

for the static tests during the present investigation. However, the behavior of the glass model in static water was studied by Reed (18) and he indicated that the bubbling for this model was very much less than that of any other nose employed in this study.

Thus, the static tests apparently indicate that surface nuclei are most effectively retained on the teflon nose under varying conditions, whereas surface nuclei are easily eliminated on the rubber nose. The other substances tested in this investigation fall in intermediate categories.

4.2 The Appearance of Cavitation at Inception and Desinence

In this section, we present some aspects of the appearance of cavitation as observed during tunnel testing. During the tests, it was found that the appearance of incipient and desinent cavitation was quite different for the various noses. Therefore, an account of the appearance of cavitation is given here in order to show a qualitative difference in the cavitation characteristics of the models.

In general, two types of cavitation were observed at inception. In some cases, it appeared to be of a continuous nature around the model nose such as for the glass and stainless steel models. In other cases, it seemed to be originating from discrete points of the surface as demonstrated by the teflon, polyethylene and rubber models. However, it should be noted that in all cases except the rubber nose, when cavitation finally occurred, it was in a state of developed cavitation rather than limited cavitation.

If we consider the results of Series A and B, we may infer that the stream nuclei are controlling the onset of cavitation for the hydrophilic surfaces such as glass and stainless steel (for an explanation of this, refer to Section 5.1). Also, for these models, we obtain a continuous ring type of cavitation which starts to flash during desinence. Therefore, these results appear to suggest that when stream nuclei are responsible for the onset of cavitation, we obtain a ring type of cavitation. On the other hand, the results of Series A and B, discussed in Section 5.1, suggest that teflon and polyethylene, which are hydrophobic, seem to depend on surface nuclei for the onset of cavitation. For these models, we observed finely separated but distributed streaks of cavitation all around the nose which became very spotty at desinence. (The spotty nature at desinence can be understood from the fact that a material contains an aggregate of very small cavities distributed throughout the volume of the substance. Some of these cavities may be quite large and some relatively small. Thus, at higher pressures, only the larger cavities may be in a position to contribute to cavitation and, hence, the spots.)

For the tests in Series C, we notice that the air content of the water was very high and also from the results of the tests, as discussed in Section 5.1, it appears that stream nuclei may be responsible for the onset of cavitation for all the noses. Therefore, based on the arguments of the preceding paragraphs, we should observe only one type of cavitation on all the noses in Series C; i.e., a continuous ring type of cavitation. But in practice, the streak type

of cavitation was observed for the teflon and polyethylene models in Series A, B, and C. Thus, the relationship between the visual appearance of the cavitation and the type of nuclei causing the cavitation is unknown.

The cavitation characteristics of various noses have been roughly sketched in Figures 12 through 17 and summarized in the following paragraphs. (The front side in these figures refers to the side of the test section or model shown in Figure 1, whereas the opposite side is called the back side.)

It should be noted in Figures 12 through 17 that the inception of cavitation corresponds to a steady state free stream pressure, P_∞, of about 5.4 psia after the tunnel was started at a set pressure of 15.3 psia. This means that the condition of inception as shown in these figures might not have been observed in that form, for all the models, exactly at the onset of cavitation. Similarly, for desinence, the various locations of spots are the totality of the spots observed for a model during all the tests. But, during any particular run or test, only one or two or more spots may have been observed.

4.2.1 Glass Hemispherical Nose (G1). For reasons to be explained in Chapter V, the glass nose was tested at an angle of attack of 5 degrees. Therefore as would be expected, cavitation was observed only on the upper face of the nose (see Figure 12).

At inception, the cavitation was quite dense and continuous as sketched in Figure 12-a. During a desinence run, the cavitation started flashing early in the run and continued doing so as the pressure was increased.

4.2.2 Stainless Steel Hemispherical Nose (S1). For this nose, cavitation inception was almost continuous in the form of a ring around the nose. This ring did not originate at the tangent point but was shifted a little towards the downstream end. (The Tangent Point of the model is the point where the hemispherical nose joins the cylindrical portion of constant cross section.)

As the pressure was gradually increased during a desinence run, the cavitation ring started flashing. Near the final stage of desinence the flashing was not present all over the nose but only near the bottom portion of the backside. The nature of cavitation for this nose is sketched in Figure 13.

4.2.3 Polyethylene Hemispherical Nose (P1). The appearance of the cavitation on the polyethylene nose was different from that of the glass and stainless steel models. At the inception of cavitation, some spots appeared near the top or bottom face on either side of the nose and quickly spread all around the nose. Though the cavitation was observed all over the nose, it was not continuous as in the case of either the glass or stainless steel models. On the contrary, there were very thin streaks of cavitation at discrete points. The points of origin of these streaks also did not lie in one vertical plane. Some were located near the tangent point and some at points upstream of the tangent point as indicated in Figure 14-a. The location of spots at the tangent point or upstream of it were quite random.

During desinence, the cavitation was very spotty. Sometimes only one spot of cavitation disappeared, whereas at other times two or more spots disappeared together. In Figure 14-b, the positions of seven spots have been sketched. However, it should be noticed that in no single run or test were all of these spots observed together. Thus, desinent cavitation with this nose was quite random in nature with respect to the location of the spots.

4.2.4 Teflon Hemispherical Noses (T1 and T2). Figures 15 and 16 show the cavitation characteristics of the two teflon noses. These noses have almost the same characteristics as the polyethylene nose so far as the appearance of cavitation is concerned. The only difference is the number and location of cavitation spots for desinent cavitation.

While testing the teflon #2 nose at higher values of the total air content, a perculiar phenomenon was observed. Besides having the usual streaks of cavitation near the tangent point, there were very tiny spots of cavitation all over the upstream portion of the nose except right at the tip. During desinence, these tiny spots disappeared before the big streaks disappeared completely.

4.2.5 Rubber Hemispherical Nose (R1). Of all the models tested, the rubber nose appeared to exhibit the most random behavior. Unlike the other noses, it was the only nose which showed a random behavior during incipient cavitation. Firstly, it was very spotty which means that a continuous ring of cavitation was never observed with this model. Secondly, sometimes a spot or two appeared on the back side while, at

other times, some spots were observed only on the front side. Eight locations of cavitation spots are shown in Figure 17-a for this nose. However, it should be noted that all of these spots never appeared in the same run or test.

In the same manner, desinence was very random for this nose. Sometimes one or two spots would remain fixed until disappearance while, at other times, flashing of cavitation in some region of the nose was observed. Also, the locations of the spots varied from run to run and/or test to test. The various spots of cavitation which were observed at different times are sketched in Figure 17-b.

4.2.6 Zero Caliber Ogive Noses (T01 and R01). Incipient cavitation was in the form of a developed cavity. As the pressure was gradually increased during desinence, the cavity became shorter and finally started flashing near the pressure corresponding to final disappearance.

With the teflon nose, during desinence at the higher value of dissolved air content (test #655) it was observed that after the cavity disappeared, some very small bubbles were present at the sharp edge of the nose. When the pressure was further increased slowly, these bubbles finally disappeared at a much higher value of the free stream pressure.

CHAPTER V

EXPERIMENTAL RESULTS

5.1 Investigation of Incipient Cavitation

5.1.1 Presentation of the Data. The experimental data are tabulated in Tables 3 and 4. For the most part, Table 3 contains information about initial conditions for all of the tests, whereas the observed data together with some calculated parameters are given in Table 4.

The various quantities tabulated in Tables 3 and 4 are defined in Table 1. For example column four in Table 4 is the inception time for the first inception run In most cases, two tests were conducted with each model and so the tabulated value of inception time is the average of the two observations. In most cases, the spread about the mean value was small.

The data are tabulated in four groups in Table 4. The first group consists of the hemispherical-nosed models with hydrophobic surfaces, such as teflon and polyethylene. Glass and stainless steel, being hydrophilic, are in the second group. The rubber hemispherical nose has been placed in a third group because of the exceptional characteristics displayed by this material. The last group consists of the zero caliber ogive noses made of teflon and rubber.

Initial tests conducted with the glass nose at an angle of attack of zero degrees indicate that the model had a very low cavitation number for the onset of cavitation, and that the pressure was too low for satisfactory operation of the tunnel. It was thus necessary to operate this model at an angle of attack of five degrees in order to increase the pressure for inception and thereby avoid unsatisfactory operational conditions.

It was difficult to run tests for prolonged periods at low pressures in Series C because of the accumulation of a multitude of bubbles caused by the high total gas content of the water. This condition made it difficult to obtain desinent cavitation data for the glass and stainless steel noses. The values of the desinent cavitation numbers for other noses and for test Series A and B have been noted in column eleven of Table 4 for future reference and for comparison with other investigations.

In Table 4, emphasis has been placed on the data for the first inception run (which is also the first run of the test) because this was the run which was most likely to show an effect of initial conditions. For example, in the case of the teflon hemispherical nose for Series B, the condition of minimum surface nuclei may only exist for the first run. This may not be true for the subsequent runs, because a continued exposure of the surface to very low pressures during the first inception run may disturb the surface nuclei situation which in turn could influence the inception time.

5.1.2 Discussion of the Results for the Hemispherical Models (T2, P1, G1, S1 and R1). A direct comparison of the inception time for the first run, column four in Table 4, for the hydrophobic models indicates that these times are small for Series A tests. However, the inception times almost double for these models in Series B. Thus, this difference in inception time should correspond to the change in the condition of surface nuclei (in Series A, the surface nuclei were maximum whereas a condition of minimum surface nuclei was characteristic of Series B). Similarly, for the first inception run a comparison of inception time for the glass and stainless steel models indicates that the magnitude of inception time does not differ significantly for Series A and B. In other words, conditioning of the surface nuclei has no effect for these substances and the corresponding time should be indicative of the stream effect on the onset of cavitation. Thus, we find that in the case of hydrophobic surfaces, surface nuclei are apparently playing an important role in the onset of cavitation under certain circumstances, whereas hydrophilic surfaces may depend entirely on the stream for nuclei.

Comparing the values of inception time, for the first inception run, for the teflon and polyethylene models in Series B and C, we find that these values are, for tests in Series C, almost half of those in Series B. This difference should then correspond to the change in the stream conditions because, for both test Series B and C, surface nuclei were kept at minimum and only the stream conditions were varied. Similarly, the inception time for the glass and stainless steel models

in column four of Table 4 is considerably smaller for Series C as compared to Series A and B. This indicates that the onset of cavitation for these two substances more or less depends on the stream As a result, the inception time is nearly the same for both Series A and B (where stream conditions were the same) and it changed in Series C (where stream conditions were altered) On the other hand, for the teflon and polyethylene models, surface nuclei were active for the onset of cavitation when surface conditions were favorable (in Series A) but the stream apparently controlled the inception when surface nuclei were reduced to a minimum (in Series B and C). The smaller values of inception time obtained in the tests of Series C may be due to the high air content of water employed in these tests. If stream nuclei were responsible for the onset of cavitation, then it may suggest that the probability of having a large number of free gas bubbles is increased thereby resulting in a decrease in the inception time. On the other hand, a high degree of over saturation as a result of the high air content may cause a rapid growth of the surface nuclei. Therefore, it is also possible that surface nuclei may influence the onset of cavitation for the teflon and polyethylene models in Series C. However, at present, it is difficult to conclude in favor of either surface or stream nuclei as the primary source for these cases.

When we compare the inception time for the first inception run in Series C for the hydrophobic (i e., teflon and polyethylene) and the hydrophilic (i e , glass and stainless steel) substances, we find that they are smaller for the former substances than for the latter

substances. This may indicate that apart from the stream, the model surfaces, too, exhibited some influence (a similar argument was presented in Section 4.2). These differences may be due to various factors such as surface smoothness, nose shape, surface characteristics, or various combinations of these possibilities.

No discussion of inception data for the rubber model was presented in the preceding paragraphs because of its perculiar surface characteristics. We find from column four of Table 4 that the comparison of inception time for Series A, B, and C for this nose shows an apparent effect of both surface and stream nuclei. The inception time is maximum for Series B. This means that as a result of minimizing the surface nuclei (from test Series A to B), the inception time went up. On the other hand, by increasing the total air content (i.e., from Series B to C) but keeping the surface nuclei to a minimum, the inception time went down. Therefore, although the trend in the data is similar to the hydrophobic substances (i e., teflon and polyethylene), it cannot be included in the same category because the magnitude of the inception time is much greater for the rubber model. The higher values of inception time might have been caused by errors in the contour of the nose (which might have caused a decrease in the minimum pressure coefficient for this model) or due to some other unknown phenomenon, but at this stage it appears difficult to conclude anything definitely.

In the previous discussions, we have focused our attention on the first inception run data. Next, we discuss the history aspect of various tests as further runs were conducted. Column five in Table 4

lists the inception time for the second run of each test, whereas in column six are listed the average values of two to six inception runs (after the first) for every test. Therefore, the comparison of values in columns 4, 5, and 6 for each test indicates that the values lie within $\pm$ 0.3 seconds of the average value and thus this shows that the results are very consistent and repeatable. The only exception to this is the teflon nose in the Series B tests. For this model, the inception time was large for the first run but suddenly dropped in the subsequent runs. However, it should be noted that teflon is the only material which does not lose all of its surface nuclei under various conditions as indicated by the static tests (refer to Section 4.2). Therefore, when the teflon model was conditioned for minimum surface nuclei in Series B, it may be that this conditioning was effective during the first run and, when subsequent runs were conducted, the surface nuclei had become active because of the low pressure conditioning in the first run.

Thus, we see that the experimental procedures gave consistent effects from one run to the next and also from one test to the next. If initially surface nuclei were active (test #311, 312 and 294, 295), the effect of such nuclei was maintained and if the stream nuclei were controlling the onset of cavitation, running time did not influence the effect of such nuclei.

Considering the effect of pressurization at 85 psia for 10 minutes prior to an inception run on the onset of cavitation (refer to columns five to seven in Table 4), we observe that for the teflon model

(where surface nuclei played an important role in inception) and for the glass and stainless steel models (where stream nuclei were the controlling factor), there was no appreciable effect of this level of pressurization. But a significant effect at the above level of pressurization is noticed for the polyethylene nose when it was tested in Series A (test #294 and 295). We observe that for this model the inception time is nearly constant at about 3.18 ± 0.14 seconds in columns four to six in Table 4 for Series A and these tests indicate that surface nuclei are contributing to the onset of cavitation. But when a pressure of about 85 psia was applied for about 10 minutes, the inception time increased to 5.03 seconds (see column seven, Table 4). This may suggest that, as a result of the pressurization, the condition of the surface nuclei was altered. When we refer to the static tests for this model, we find that, as a result of pressurization in water at 80 psi for 10 minutes, this material tends to lose its surface nuclei (refer to Section 4.1). But the same is not true for the teflon model when subjected to 85 psia for 10 minutes. This may be caused by differences in porosity. Teflon is comparatively more porous than polyethylene, so that the former may have a larger supply of gas in the pores which could not be completely eliminated by pressurization. But, polyethylene being less porous may have a smaller amount of gas and thus may be more influenced by pressurization.

The inception data for the rubber nose, from Table 4, is noted below:

2 Test Series	3 Model	4 t_{i-1}	5 t_{i-2}	6 t_{i-av}	7 t_{i-pav}
A	R1	9.60	8.31	12.49	12.30
B	R1	10.14	8.02	8.33	10.90
C	R1	7.86	2.82	3.52	5.54

We observe that it is not consistent as was the case with the other models. From the data, it appears that the inception time falls in the second run but again increases for subsequent runs in almost all the tests for this model. Data in column seven also indicates that there may be an effect of pressurization at 85 psia for 10 minutes prior to an inception run as well, but again it is not true for the tests in Series A for this model. Thus, at present, it appears to be difficult to conclude anything definite about this model.

5.1.3 The Meaning of Inception Time for Surface and Stream Nuclei. In this section, we are interested in discussing the meaning of the inception time observed in various tests and discussed in the preceding section. We observed that for the teflon and polyethylene models, surface nuclei contribute to the inception of cavitation in certain circumstances (i.e., for the tests in Series A) and for those cases, the inception time was 2.99 ± 0.33 seconds. In the case of the glass and stainless steel models, stream nuclei seem to be influencing the onset of cavitation and the inception time can be taken as 6.00 ± 0.60 seconds for Series A and B tests.

The inception time for the surface nuclei, namely, 2.99 ± 0.33 seconds, may correspond to the time taken by the gas bubbles trapped in the pores of the material to grow to a significant size. On the other hand, the inception time of 6.00 ± 0.60 seconds for the stream nuclei may be a characteristic time for the pump-tunnel combination of the experimental facility. This time may be that required by the water to pass through the pump-tunnel circuit a characteristic number of times before enough bubbles are created in the stream to give rise to cavitation. It is interesting to note that at a velocity of 39 fps in the test section a particle will traverse the tunnel along the central streamline in about six seconds.

The inception time for test Series C is 2.65 ± 0.35 seconds for the hydrophobic surfaces and is given by 3.80 ± 0.75 seconds for the hydrophilic surfaces When these values are compared with those of Series B tests, we find that these are much smaller. This decrease in the inception time may be due to the higher total air content characteristic of test Series C

5.1.4 Vaporous and Caseous Cavitation. For the inception runs noted in Table 4 and discussed in Section 5.1.2, the tunnel was started at a set pressure of 15.3 psia so that steady flow was attained at a pressure of 5.4 psia and a velocity of 38.8 fps which gave a cavitation number of 0.48 (note that the minimum pressure coefficient for the hemispherical models is 0.69). This implies that the cavitation was vaporous at steady state. Except for the rubber nose the cavitation was usually well developed at the steady state condition because of the

low cavitation number. However, we observe that in some cases cavitation was initiated long before the steady state was attained. For example, in test #311 and 312 with the teflon model, the inception time is only about 2.75 seconds. This inception time is much less than the calibration time for the tunnel which was about 8.4 seconds (the calibration time is the time taken by the tunnel to reach a steady state after it was started). The minimum pressure on the model nose at the moment of cavitation initiation was 3.95 psia. This indicates that at the time of initiation, cavitation was not vaporous but rather it was gaseous. Similar arguments can be advanced for the polyethylene nose (additional aspects concerning gaseous cavitation on these models are discussed in Section 5.2).

In the case of the stainless steel model, the situation was somewhat different. For this model, the minimum pressure on the model nose was below the vapor pressure at cavitation initiation as indicated by a surface pressure of about -1.1 psia at the minimum pressure point in Series A and B.

It is important to note the difference in the nature of the appearance of cavitation at initiation for the hydrophobic models (i.e., teflon and polyethylene) and the hydrophilic models (i.e., glass and stainless steel). For the former, cavitation would initially appear at one or two points on the nose and then quickly spread over the whole surface in the form of developed cavitation. In the case of the hydrophilic substances, the appearance of cavitation at initiation was not very much different from its final state as seen by the naked eye

5.1.5 Discussion of the Results for the Zero Caliber Ogive Noses (TO1 and RO1). For convenience, we note the data for the zero caliber ogive models from Table 4 in the following form:

2 Test Series	3 Model	4 t_{i-1}	5 t_{i-2}	6 t_{i-av}
A	TO1	2.51	2.51	2.47
A	RO1	2.74	3.31	4.76
B	TO1	4.37	2.92	3.02
B	RO1	5.59	2.74	2.72
C	TO1	2.33	2.35	2.33
C	RO1	2.47	2.40	2.42

A comparison of the inception time for the first inception run for Series A and B suggests an effect of surface nuclei (note that surface nuclei were maximum in Series A while they were minimum in Series B). Similarly, a comparison of Series B and C tests suggests that stream conditions also show a significant effect and that as the total air content increases, the inception time goes down (note that the total air content of water was increased considerably in going from Series B to C)

Thus, from the experimental data, it appears that both the surface nuclei and the stream nuclei may be active in different circumstances. But from an understanding of the flow characteristics of the zero caliber ogive noses, we would not expect any major contribution from the surface of the model and the model should depend primarily on the stream for nuclei. Therefore, the interpretation of the data for the zero caliber ogives is indefinite at this time.

5.1.6 Comparison with Previous Investigations. Before an attempt is made to compare the results of this investigation with those of Treaster (20), Holl and Treaster (14) and Reed (18), one important fact should be clearly noted. In previous investigations, the most important quantity for comparison was the delay time, whereas in this investigation, emphasis has been placed on inception time. However, this difference in emphasis may not be very critical because inception time does represent a measure of the delay in cavitation during the inception process.

Treaster found a marked decrease in delay time for the stainless steel model when it was coated with teflon and he attributed this to the hydrophobic and porous nature of the teflon coating. Similarly, Reed, and Holl and Treaster observed no delay time with the solid teflon surface. The results of this study also indicate that solid teflon is the only substance which shows the maximum contribution from the surface nuclei and the inception time is also very small. However, Reed's conclusion concerning the effect of pressurization of the teflon model appears to be contradicted, to some extent, by the present study. Whereas Reed found no effect of pressurization at 750 psia for 50 minutes, an initial effect of pressurization was observed in the first inception run of tests #560 and 561 with the solid teflon nose during the present investigation. This may be due to the fact that pressurization was more severe in the present investigation since pressures of 291 to 1000 psi were employed for periods of 41 to 48 hours. However, the application of a pressure of 85 psia for 10 minutes prior to an inception run showed no significant effect during this investigation.

Reed did not observe pressure history effects for the teflon nose but did experience such effects in many other instances. However, it is not clear how these effects can be related to the present investigation because different facilities and procedures were used. Many of Reed's pressure history effects may have been due to changes in the distribution of stream nuclei which depends in general on the characteristics of the flow facility.

Comparing the data for the glass and stainless steel noses, Reed observed relatively large values of the delay time for the glass nose whereas the inception time, during this study, was not much different for the two noses In this regard, it should be noted that, during the present investigation, the glass nose was tested at an angle of attack of 5 degrees, whereas it was at zero degrees for Reed's experiments. Therefore, whether the discrepancy is due to the angle of attack or due to some other factor is unresolved at this stage and may need to be considered further

Reed also carried out some theoretical calculations for the delay time. But neither Reed's results nor the present results appear to be explained by his calculations. However, we note that Reed employed the nuclei model of Harvey et al (11) by using the Epstein-Plesset solution (6) for diffusion into a conical cavity. For this solution, one of the important assumptions made is that the diffusion length is much greater than the bubble or cavity diameter. This may not be true for the cases considered by Reed and this question should be resolved.

5.2 Investigation of Gaseous Cavitation

5.2.1 Introduction In the investigation of limited cavitation, inconsistencies between various sets of data taken under supposedly identical conditions have been encountered. It is the contention of Holl (13) that this may often be due to the improper identification of flow regimes. That is, in investigating a certain flow, an observer may feel that he is observing vaporous cavitation but in reality the cavitation is gaseous. Since vaporous and gaseous cavitation are controlled by different mechanisms, it is understandable that such confusion can lead to inconsistencies in various sets of data.

Early in this investigation, it became apparent that the teflon and polyethylene models both of which are hydrophobic experienced gaseous cavitation quite easily. Furthermore, such cavitation could be produced at flow states where the boundary pressure was significantly above vapor pressure. It was thus decided to conduct special tests which were specifically designed to investigate both desinent and incipient gaseous cavitation. The results of the desinent gaseous cavitation tests are presented in the following section whereas the incipient gaseous cavitation data are given in Section 5.2.3.

5.2.2 Desinent Gaseous Cavitation Just prior to the disappearance of all cavitation on the teflon and polyethylene models only one or two small spots of cavitation were observed during this investigation. In most cases, these spots remained in fixed positions during a particular run.

Because of the experience of Holl (12) with spots of gaseous cavitation, the behavior of the teflon and polyethylene models suggested that the spots of cavitation were gaseous cavitation rather than vaporous cavitation. Therefore, some additional tests, namely, #308, 564, and 295, were specifically designed for the study of gaseous cavitation and carried out with the teflon and polyethylene noses. Desinent cavitation runs were carried out at both speeds namely 29 fps and 39 fps. The results of these tests are noted in Table 5. However, in order to exhibit the repetitiveness of the desinent numbers in different tests, the results of other tests, namely, #294, 309, 562, and 563, have also been noted in Table 5.

In order to compare the experimental values of desinent numbers with the calculated values, Equation (13) of Reference (12) was employed:

$$\sigma_d = C_P + \frac{\sigma_d \beta}{1/2\ \rho_L\ V_\infty^2} \qquad (5.1)$$

The term corresponding to the reciprocal of Weber Number (We) has been neglected in the above equation. [Note that, by definition, Weber Number is equal to the ratio of inertia forces to surface tension forces. Also see page 144 of Reference (15).]

The pressure coefficient, C_P, in Equation (5.1) is to some extent indefinite. In most instances, spots of cavitation were stabilized near the region of minimum pressure and therefore as an estimate, C_P may be taken as equal to C_{Pmin} for a hemispherical nose which is 0.69 for the cases considered. However, Holl (12), for his

calculations, employed the cavitation number σ_p, corresponding to the disappearance of areal vaporous cavitation at the highest speed during the particular test). Similarly, during the present testing, a value of σ_p equal to 0 877 for the teflon model and σ_p equal to 0 804 for the polyethylene model, at the higher speed of about 90 fps and corresponding to the beginning of the spotty appearance of cavitation were recorded. However, the values of σ_p were not easily obtained because the disappearance of the areal cavitation was not well defined as in the cases considered by Holl

Equation (5 1) is plotted in Figures 18 and 19 for two values of the dissolved air content, and these results are shown by the curves numbered 3, 4, 7, and 8 Two values of C_P have been considered, namely, one equal to σ_p and the other equal to C_{Pmin} It is observed that the theoretical curves agree more closely with the experimental values at the higher air contents The rather poor agreement at lower values of the air content suggested the use of the term involving Weber Number in Equation (5 1), so that with this term, the equation takes the form

$$\sigma_d = C_P + \frac{\alpha_d \beta}{1/2\ \rho_L\ V_\infty^2} - \frac{2\gamma/r}{1/2\ \rho_L\ V_\infty^2} \qquad (5\ 2)$$

Equation (5 2) has been plotted in Figures 18 and 19 for two values of r (the bubble radius at final detinence), namely 3 33 x 10^{-4} and 2.0 x 10^{-4} inches, and these results are given by the curves numbered 1, 2, 5 and 6 The agreement of Equation (5 2) with the

experimental values for lower air contents is better than that of Equation (5.1), but Equation (5.1) is in better agreement with the data for higher values of the dissolved air content.

It is observed from Figures 18 and 19 that the theoretical results agree very well with the experimental results at higher dissolved air contents without the Weber Number term. Whereas, the agreement at lower values of air content is good with the Weber Number term included. This might suggest that the value of the bubble radius at the disappearance of cavitation is much greater at higher values of air content than at lower air contents. However, from physical understanding and visual observations during testing, it is difficult to say whether this is in fact true.

It should be noted that in applying Equations (5.1) and (5.2), it was assumed that the dissolved air content, α_d, was equal to the total air content, α, as measured by the Van Slyke apparatus. This assumption may be somewhat questionable in cases where the percentage of free air is high and thus may account for some of the lack of agreement between theory and experiment in Figures 18 and 19.

5.2.3 Incipient Gaseous Cavitation. Incipient gaseous cavitation was studied with the teflon #1 model and the experimental results of this study have been summarized in Table 6. We note that in this table three values of time, namely, the inception time, calibration time and delay time have been listed in columns five to

seven. The first two values were used to calculate the third with the help of the following relation:

$$t_d = t_i - t_{cal} \quad . \tag{5.3}$$

Thus, we note that in some instances the value of delay time as given by Equation (5.3) is negative. It should be emphasized that the calibration time for this investigation was much greater than the drop time for Reed's (18) study (drop time is the time required to drop the pressure from a high value to the inception value with the tunnel running at steady state). The pressure in the test section and over the model surface was also continuously dropping during the calibration time. Thus, the cases which give negative values of delay time are those for which cavitation was initiated before the set value of the inception pressure was reached.

The value of C_{Pmin} equal to 0.69 was employed to calculate the minimum pressure on the model nose from the corresponding value of free stream pressure at inception, P_{∞_i}. This value of minimum pressure was taken equal to the liquid pressure for delay time calculations presented in the latter part of this section.

It is interesting to note that when the value of inception pressure was very close to the desinent pressure (run #20, test #308), no cavitation was observed during a period of 300 seconds for which observation was made. But as the inception pressure was lowered, finite values of delay time were obtained. This implies that as the relative saturation increases, the delay time decreases. Similarly, for test #309, since the relative saturation was small, namely about

1.7, very high delay times were observed. The trend of increasing delay time with increasing inception pressure (and hence decreasing relative saturation) is also obvious from the data of test #564.

The Henry's Law constant, β, is approximately 1 psi/ppm at the temperatures employed in this investigation. Thus, the relative saturation at the minimum pressure point in the absence of surface tension is approximated by the ratio of the air content in Table 3 to the corresponding minimum pressure in column four of Table 6.

Another important observation to be made in Table 6 is the effect of air content on delay time. We note from Table 3 that the air content for test #564 was much greater than that for either test #308 or 309. Therefore, even though higher values of inception pressure were employed in test #564, very short values of delay time or inception time were obtained. All the runs presented in Table 6 were conducted at the higher speed of about 39 fps.

Column eight has been incorporated in Table 6 merely to present a qualitative summary of cavitation characteristics of the incipient gaseous cavitation as distinguished from the vaporous cavitation discussed in Sections 4.2 and 5.1.

In order to find out whether or not the observed values of delay time were of some significance, some very simple calculations were carried out by employing the Epstein-Plesset solution (6) to the nuclei model of Harvey et al (11). At this stage it should be noted that there is a significant difference between the mechanisms of vaporous and gaseous inception of cavitation. For the former, the rapid growth is due to the fast conversion of a liquid to its vapor

form whereas for the latter, growth essentially occurs due to the relatively slow rate of transport of noncondensable gas to the cavitation nuclei. It takes place only due to a high degree of over saturation of the liquid. Reed (18) carried out some calculations for incipient vaporous cavitation but his results did not explain the experimental findings. On the other hand, some of the basic equations as used by Reed were employed during this study in order to estimate the delay time for incipient gaseous cavitation. It was found that it is possible, even with the great degree of simplification used in these calculations, to obtain growth times of the same order of magnitude as observed during the tests. The equations employed were:

$$3(1-\epsilon^2) + 2\delta\left[\frac{3}{1-f} - 2\right](1-\epsilon) + \frac{2\delta^2}{1-f}\left[\frac{3}{1-f} - 2\right] \ln \frac{(1-f) - \delta}{\epsilon\,(1-f)-\delta} = (1-f)\,\frac{H_s}{H_v}\,x^2, \qquad (5.4)$$

where

$$\frac{H_s}{H_v} = -\frac{6\left[1 - \sin(\theta - \Phi)\right]}{\cos^3(\theta - \Phi)\cot\Phi + \sin^3(\theta - \Phi) - 3\sin(\theta - \Phi) + 2} \qquad (5.5)$$

$$\epsilon = \frac{R}{R_o}\,, \qquad (5.6)$$

$$\delta = \frac{2\gamma}{P_L - P_v}\,, \qquad (5.7)$$

$$f = \frac{\beta C_i}{P_L - P_v}\,, \qquad (5.8)$$

$$x^2 = \frac{2D\,R_s\,T}{\beta\,R_o^{\,2}}\,t\,, \qquad (5.9)$$

and

Φ = half angle of the conical cavity.

P_L used in the above equations is the liquid pressure outside the cavity and is equal to P_{min_i} given in column four of Table 6.

Equations (5.4) and (5.5) have been altered to account for the fact that θ was greater than 90 degrees whereas in the cases considered by Reed, θ was less than 90 degrees.

The basic geometrical factors employed in Equation (5.4) to Equation (5.9) are defined in Figure 20. It is assumed that the nucleus has some initial size measured by R_o. Growth occurs due to the transport of noncondensable gas across the interface causing the interface to move outwards. The pressure P_{min_i} must be such that the liquid is supersaturated for growth to occur. Also, it is noted that the surface tension acts in the direction opposite to that for a bubble. This fact influences the terms involving δ in Equation (5.4). In order to carry out a calculation based on Equation (5.4), it is necessary to select an initial radius, i.e., R_o and some final radius, i.e., R_f so that ϵ is specified. It is realized that R_o and R_f are indefinite. Nevertheless, R_f may possibly be estimated by assuming it to be equal to the lower limit of size visible to the naked eye, i.e., about 0.001 inches. Thus, R_o would be several orders of magnitude smaller than R_f.

For carrying out some calculations in this study, three values of initial radius, R_o, were considered, namely, 10^{-6}, 10^{-5} and 10^{-4} inches, and time for the growth of interface radius five to fifty times

the initial value were calculated for various values of half cavity angle, Φ. For each of such calculations, the value of liquid pressure, P_L, was kept constant. It was found that the growth time was very much dependent on the value of initial radius. Negative growth times were obtained for some values of ϵ. The positive values of growth time obtained for some cases were then plotted as a function of Φ. One such graph is shown in Figure 21 corresponding to a liquid pressure of 0.95 psia which is the value of P_{min_1} for runs #21 to 25 of test #308 in Table 6.

In Figure 21, two curves numbered 1 and 2 have been plotted for an initial radius of 10^{-4} inches. For initial radius of either 10^{-6} or 10^{-5} inches, no positive values of growth time were obtained. This was also true for values of ϵ less than thirty at the initial radius of 10^{-4} inches. However, any number of curves for greater values of ϵ can be obtained which will occupy the region of the plot above curve number 1 in Figure 21. From this plot, we observe that the experimental values of delay time for runs #21 to 25 of test #308 lie in the region of positive growth time. But it is difficult to select any particular theoretical value for comparison with a given experimental result because ϵ and Φ are unknown.

CHAPTER VI

SUMMARY OF RESULTS AND CONCLUSIONS

6.1 Summary

The main purpose of this study was to investigate the effects of surface characteristics on the onset of cavitation. The surface characteristics of concern were the contact angle and porosity. In addition, desinent and incipient gaseous cavitation were also studied and some encouraging results were obtained.

In order to separate the effects of contact angle from those of porosity, test models made of five different materials, namely, glass, stainless steel, polyethylene, teflon and rubber were employed. Special procedures were followed for distinguishing between the effects of surface and stream nuclei. All of the cavitation tests were divided into three main categories referred to as test Series A, B and C. In Series A, a condition of maximum surface nuclei and minimum stream nuclei was obtained, whereas in Series B, both types of nuclei were minimized. Test Series C was characterized by a condition of minimum surface nuclei and maximum stream nuclei. In this way, it was easier to analyze separately the effects of the surface and the stream nuclei.

The cavitation tests were conducted in a water tunnel having a circular test section with an inside diameter of six inches. Most of

the experiments were conducted at the higher speed of 39 fps although some desinent gaseous cavitation tests were conducted at the lower speed of 29 fps.

In addition to the water tunnel experiments, tests were conducted with the various models under static conditions in various containers. The purpose of these tests was to determine the effect of various types of pressurization on surface bubbling.

6.2 Conclusions

The main conclusions which can be reached from this study are listed in the following sections.

6.2.1 Static Tests. The teflon model which was hydrophobic and porous has profuse surface bubbling initially and retains some bubbles even after pressurization with water. In contrast to this, the rubber model which is wetted by water is influenced very easily by pressurization with water for, in some cases, the surface nuclei were apparently completely eliminated by the pressurization. The other surfaces employed in this investigation namely polyethylene and stainless steel are in categories between the teflon and rubber with respect to the influence of water pressurization on surface bubbling.

6.2.2 Incipient Cavitation. (a) The hydrophobic hemispherical models made of teflon and polyethylene indicate a definite contribution of surface nuclei to the onset of cavitation provided the surface nuclei

are in a normal condition, i.e., no effort has been made to minimize the surface nuclei.

(b) The hydrophilic hemispherical models made of glass and stainless steel seem to show no contribution of surface nuclei to the onset of cavitation and may depend entirely on the stream nuclei for cavitation.

(c) The rubber hemispherical model behaved in a manner different from that of the teflon, polyethylene, glass and stainless steel models. This model may or may not have a contribution of surface nuclei to the onset of cavitation.

(d) The observations for the zero caliber ogive models are unexplained. These results suggest contributions by surface nuclei but this is difficult to reconcile with the fact that because of the nature of the separated flow the primary source of nuclei for such bodies is probably the stream.

(e) With an increase of air content an increased effect of stream nuclei is apparent from the results of test Series C. Thus, as the air content increases the inception time decreases.

6.2.3 Gaseous Cavitation. (a) The desinent number increases as velocity decreases.

(b) The desinent number increases as the air content increases.

(c) For incipient gaseous cavitation, the inception time (and hence delay time) increases as the relative saturation is decreased or as the inception pressure in increased.

(d) The inception time decreases as the air content increases.

(e) The experimental observations agree fairly well with the theoretical results for desinent cavitation indicating that the theory based on Henry's Law is a reasonable approximation of reality

(f) The comparison of the estimated cavitation delay times with experimental values for incipient gaseous cavitation suggests that the proposed theoretical model is plausible

6.3 Recommendations

As a result of the discussion presented in Chapter V and from the general observations made during this investigation, the following suggestions are advanced for future study:

(a) In order to have a better understanding of the effects of stream nuclei on the onset of cavitation, a device should be designed for measuring the number and size of the bubbles present in the stream

(b) Reed's theory for incipient vaporous cavitation predicts cavitation delay times which are considerably smaller than experimental values. This may be due to the assumption that the diffusion length is considerably greater than the cavity dimension. This point should be examined further.

(c) It was difficult to explain the trends of the inception data for the rubber nose. This may be due to a lack of knowledge of the properties of this material. Therefore, some similar materials with known properties should be tested.

(d) In all cases, it was assumed that the noses of hemispherical models were true hemispheres. Since departures from the basic shape may influence the inception time, the contours of the models should be examined. In particular, the rubber model should be examined since it did not appear to agree with the trends established by the other models.

(e) The apparent effect of surface nuclei observed for the zero caliber ogive noses on the onset of cavitation is unexplained. Therefore, similar models made of other materials should be tested in order to better explain the cavitation characteristics of zero caliber ogive noses.

(f) The theoretical calculation of the delay time for incipient gaseous cavitation is very dependent upon the initial and final size of the cavity. This question must be examined further in order to determine a rational means for selecting the size of the cavity at the beginning and end of its growth

REFERENCES

1. Bigelow, W. C., Pickett, D. L., and Zisman, W. A., "Oleophobic Monolayers. I. Films Adsorbed from Solution in Non-Polar Liquids", Journal of Colloid Science, Vol. 1, p. 513, 1946.

2. Bikerman, J. J., "Surface Roughness and Contact Angle", Journal of Physical and Colloidal Chemistry, Vol. 54, p. 1653, 1950.

3. Bikerman, J. J., The Science of Adhesive Joints, Academic Press, New York, 1961, pp. 36 and 34.

4. Brown, S. J., "The Behavior of Tap Water under Dynamic Tensile Stressing in a Non-Flow System", M.S. Thesis, The Pennsylvania State University, June 1967, Figure 6.

5. Cooper, W. A. and Nuttall, W. A., Journal of Agr. Sci., Vol. 7, p. 219, 1915.

6. Epstein, P. S. and Plesset, M. S., "On the Stability of Gas Bubbles in Liquid-Gas Solutions", Journal of Chemistry and Physics, Vol. 18, p. 1505, 1950.

7. Eurich, R. E., "The Effect of Air Content and Velocity on Cavitation Hysteresis", M.S. Thesis, University of Nebraska, May 1962.

8. Fox, H. W. and Zisman, W. A., "Some Advances in Techniques for the Study of Absorbed Monolayers at the Liquid-Air Interfaces", Review of Scientific Instruments, Vol. 19, p. 274, 1948.

9. Geller, I., "Some Physical and Chemical Properties of Carbon and Graphite Electrodes Prepared from Anthracite", Ph.D. Thesis, The Pennsylvania State University, January 1959, pp. 15-17.

10. Gould, R. F., Editor, Contact Angle, Wettability, and Adhesion, Advances in Chemistry Series, No. 43, pp. 1-51.

11. Harvey, E. N., McElroy, W. D. and Whiteley, A. H., "On Cavity Formation in Water", Journal of Applied Physics, Vol. 18, p. 162, February 1947.

12. Holl, J. W., "An Effect of Air Content on the Occurrence of Cavitation", Transactions of the ASME, Journal of Basic Engineering, Series D, p. 941, December 1960.

13. Holl, J. W., "Limited Cavitation", Symposium on Cavitation State of Knowledge, Published by The American Society of Mechanical Engineers, 345 East 47th Street, New York, N. Y. 10017.

14. Holl, J. W. and Treaster, A. L., "Cavitation Hysteresis", Transactions of the ASME, Journal of Basic Engineering, Vol. 88, Series D, No. 1, p. 199, March 1966.

15. Knudsen, J. G. and Katz, D. L., Fluid Dynamics and Heat Transfer, McGraw-Hill, New York, 1958.

16. Livingston, H. K., "Contact Angles and Absorption on Solid Particles", Journal of Physical Chemistry, Vol. 48, p. 120, 1944.

17. Raats, E., "Changes in Physical Properties of Graphite upon Gasification with Carbon Dioxide", Ph.D. Thesis, The Pennsylvania State University, June 1955, pp. 8-18.

18. Reed, R. L., "The Influence of Surface Characteristic and Pressure History on the Inception of Cavitation", M.S. Thesis, The Pennsylvania State University, March 1969.

19. Schonhorn, H. and Ryan, F. W., "Wettability of Polyethylene Single Crystal Aggregates", Journal of Physical Chemistry, Vol. 70, p. 3811, 1966.

20. Treaster, A. L., "Cavitation Hysteresis", M.S. Thesis, The Pennsylvania State University, June 1964.

APPENDIX A

HELIUM-MERCURY DENSITY METHOD FOR POROSITY MEASUREMENTS

In Section 2.1-c, we have defined porosity as the ratio of void volume to the total volume of the material. In the present investigation, only the accessible porosity was of concern as against the total porosity. This means that, for our purpose, the void volume is the volume of all the pores in the material except those which are completely blocked off (these are the pores in the body of the material which are not accessible to the exterior of the material from any side). Therefore, the true and apparent densities of the materials were measured by the helium displacement and the mercury displacement methods. These were called the helium density and the mercury density of the material and designated as ρ_{He} and ρ_{Hg}, respectively.

Mercury densities were determined by a weighing technique using a specific-gravity bottle and mercury as a displacement fluid. The sample was weighed, the weight of the specific-gravity bottle determined while full of mercury, and again determined with the sample immersed. The weight and volume of displaced mercury was thus calculated. These figures were then used to calculate the mercury density of the sample. The actual apparatus used is known as a mercury porosimeter, details of which are given on pages 8 to 18 of Reference (17).

Helium densities were determined with a constant pressure helium displacement apparatus. The principle of this apparatus is the same as explained for the measurement of mercury density. The only difference is in testing procedure and the apparatus used, further details of which are given on pages 15 through 17 of Reference (9).

The pore volume of the sample can be calculated from the reciprocals of the two densities,

$$\theta' = \frac{1}{\rho_{Hg}} - \frac{1}{\rho_{He}} , \qquad (A.1)$$

where

$$\frac{1}{\rho_{Hg}} = \frac{\text{Total volume of the sample}}{\text{Mass of the sample}} , \qquad (A.2)$$

and

$$\frac{1}{\rho_{He}} = \frac{\text{(Total volume - Pore volume) of the sample}}{\text{Mass of the sample}} \qquad (A.3)$$

Therefore,

$$P = \theta' \rho_{Hg} , \qquad (A.4)$$

or

$$P = \frac{\rho_{He} - \rho_{Hg}}{\rho_{He}} . \qquad (A.5)$$

Equation (A.5) was employed to calculate the values of porosity given in Table 2.

APPENDIX B

GONIOMETER MEASUREMENTS FOR CONTACT ANGLE

The contact angle formed by a drop of ordinary tap water on the surface was measured by a simple and convenient instrument called the telescope-goniometer (1). For this measurement, the telescope is rotated until one of the cross hairs is parallel to the solid surface. The second cross hair is then rotated with reference to the first cross hair, so as to make it tangent to the air-water interface. The angle between the cross hairs, read directly on the scale of the instrument, gives the required value of the contact angle.

For the measurements of contact angle in Table 2, test samples were made in the form of small circular disks, with flat faces, for four materials, stainless steel, rubber, polyethylene and teflon. However, no measurements could be made for pyrex-glass as its sample was not easily available. Also, all the measurements were made in the atmosphere at room temperature after cleaning the surface with methyl carbinol ACS (in place of acetone).

APPENDIX C

USE OF LUCITE CAP

During test Series A, it was required to run the tests with nearly maximum number of surface nuclei. In order to insure such a condition, it was essential to cover the nose during the deaeration and tunnel-pressurization periods. For this purpose, therefore, the lucite cap shown in Figure 5 was designed. The open end of this cap had a radial groove which housed an O-ring. The O-ring was designed to fit around the flat portion of the sting mount, and thus prevent water from entering the cap. To insure that no water actually leaked into the cap, a small amount of red dye was introduced into the cap before it was installed on the sting. Thus, if at any moment, any water entered the cap, this condition would at once be indicated by the red color of the water which had leaked into the cap.

APPENDIX D

PRESSURE RESPONSE CURVES

During the inception runs, one of the difficulties encountered was noting the exact value of the inception pressure, P_{∞_i}. The reason was that, in most cases, cavitation would appear before the tunnel attained a steady state. The only values of the pressure which could be easily noted were the lowest pressure reached which corresponded to the steady state of the tunnel and the initial value of the set pressure. Therefore, it was necessary to find an indirect method of calculating the value of inception pressure. The best reference for this was obviously the inception time. Thus a pressure response curve was established for the tunnel-gauge system. The time taken by the pressure to fall to 14 psia, 13 psia and so on, from a fixed set pressure of 15.3 psia, was recorded and checked with the help of a pressure transducer. From this data, a curve of P_∞ versus time was constructed as shown in Figure 7. In this way, for any given t_1, the corresponding value of P_∞, from this plot, gave the required value of P_{∞_i}.

From Figure 7, a graph of minimum pressure (on the nose of the hemispherical model) against time was constructed as shown in Figure 8.

This was easily obtained after the plot of P_∞ versus P_{min} was drawn by using the equation:

$$C_{Pmin} = \frac{P_\infty - P_{min}}{1/2\ \rho_L\ V_\infty^2} \quad , \tag{D.1}$$

or

$$P_{min} = P_\infty - 1/2\ \rho_L\ V_\infty^2\ C_{Pmin} \quad . \tag{D.2}$$

It is to be noted in Equation (D.2) that velocity is not constant. It is given, at any value of P_∞, by:

$$P_s - P_\infty = 1/2\ \rho_L\ V_\infty^2 \quad . \tag{D.3}$$

Velocity is shown as a function of P_∞ in Figure 10. Employing Equation (D.3) in Equation (D.2) yields:

$$P_{min} = P_\infty\ (1 + C_{Pmin}) - P_s\ C_{Pmin} \quad , \tag{D.4}$$

or

$$P_{min} = 1.69\ P_\infty - 15.3\ C_{Pmin} \quad . \tag{D.5}$$

The value of C_{Pmin} for the corresponding Reynolds Number of 8.75×10^4 (based on model diameter) was 0.69.

Equation (D.2) was directly employed for calculating P_{min} for various values of P_∞ corresponding to a steady state average velocity of 38.82 fps. This plot of P_{min} versus P_∞ is given in Figure 11.

TABLE 1

NOTATIONS FOR TABLES 2 THROUCH 6

A, B, C	names of the test series
C_{Pmin}	minimum pressure coefficient for the hemispherical-nosed models
G1	1/4" glass hemispherical-nosed model #1
P	porosity cc/cc
P1	1/4" polyethylene hemispherical-nosed model #1
P_{∞_i}	free stream static pressure in the test section corresponding to the inception of cavitation, psia
$P_{\infty_{i-1}}$	free stream static pressure in the test section for the #1 inception run and averaged for the corresponding tests indicated in the first column, Table 4, psia
P_{min_i}	pressure at the minimum pressure point of the nose at inception, psia
$P_{min_{i-1}}$	average value of the minimum pressure on the hemispherical nose for the #1 inception run of the corresponding tests in column 1, Table 4, psia
P_s	set pressure for inception runs, psia
$\bar{P}_v$	average value of vapor pressure, averaged over all tests, psia
R1	1/4" rubber hemispherical-nosed model #1
RO1	1/4" rubber zero caliber ogive #1
S1	1/4" stainless steel hemispherical-nosed model #1
T1	1/4" teflon hemispherical-nosed model #1

T01	1/4" teflon zero caliber ogive #1
T2	1/4" teflon hemispherical-nosed model #2
t_{cal}	calibration time, seconds
t_d	delay time for the inception run, seconds
t_i	inception time, seconds
t_{i-1}	average value of inception time for #1 inception runs of corresponding tests in column one, Table 4, seconds
t_{i-2}	average of inception time for #2 inception runs of corresponding tests in column one, Table 4, seconds
t_{i-av}	average value of the inception time for two to six inception runs following the #1 inception run for corresponding tests in column one, Table 4, seconds
t_{i-pav}	inception time for inception runs carried out after pressurizing the system normally at 85 psia for 10 minutes prior to each of these runs and averaged for the corresponding tests in column one, Table 4, seconds
V_∞	free stream velocity in the test section, ft/sec
$\bar{V}$	average test section velocity for all of the tests, ft/sec
α	total air content of water, ppm
α'	angle of attack, degrees
ρ_{He}	helium density of the material, gm/cc
ρ_{Hg}	mercury density of the material, gm/cc
$\bar{\sigma}_d$	average value of the desinent cavitation number
σ_{i-1}	average value of the incipient cavitation number for the corresponding tests in column one, Table 4, and corresponding to the #1 inception runs
θ	contact angle, degrees

TABLE 2

SURFACE CHARACTERISTICS OF THE TEST MODELS

Test Model	Nose Material	Contact Angle		Material Densities **		p	Wettability with Tap Water
		Measured * (degrees)	Tabulated (degrees)	ρ_{He} gm/cc	ρ_{Hg} gm/cc	cc/cc (percent)	
1/4" Glass Hemisphere #1	Pyrex-Glass (Corning Code #7740)	-	Zero (16)	-	-	Nil'	Wets
1/4" Stainless Steel Hemisphere #1	Stainless Steel (Type 416)	81	60-94 (2)	8.137	7.700	5.4	Wets
1/4" Rubber Hemisphere #1 and 1/4" Rubber Zero Caliber Ogive #1	#400 Pink Pearl Eraser ** (Eberhard Faber Co.)	110	-	1.650	1.410	14.5	Wets +
1/4" Polyethylene Hemisphere #1	Solid Polyethylene (Low Density)	102	93, 99 (19) (3)	0.799	-	1-2'	Does Not Wet
1/4" Teflon Hemispheres #1 and #2 and 1/4" Teflon Zero Caliber Ogive #1	Solid Teflon (Type "TFE") ++	123	110 (8)	2.413	2.200	8.8	Does Not Wet

' These are approximately the probable values.

** This eraser is a combination of a rubber substitute used as a binder; pumice used as an abrasive and factice used as the cleaner. This is extruded, chopped and vulcanized.

* These measurements were made by the goniometer in the laboratory of the Department of Mineral Preparation at The Pennsylvania State University, employing ordinary tap water over dry surfaces (See Appendix B).

** Measured in the Laboratory of the Department of Mineral Sciences at The Pennsylvania State University by the helium displacement and the mercury displacement methods (See Appendix A).

+ Although the contact angle for this material is greater than 90 degrees, water appears to wet the surface. This may be explained by the fact that contact angle is not the only measure of wetting (See Section 2.2).

++ "TFE" type of teflon is hydrophobic, opaque, and made by powder metallurgical techniques, i.e., a cintering process. Its porosity is slightly higher than the "FEP" type of teflon and is not as uniform as for the "FEP" type which is made by a molding process.

TABLE 3

INITIAL CONDITIONS FOR THE TESTS

Date	Test No.	Time for the Test (minutes)	Model	Maximum Surface Nuclei (Model in Air) Pr. (psi)	Time (hrs.)	Minimum Surface Nuclei (Model in Water) Pr. (psi)	Time (hrs.)	Max. Stream Nuclei	TUNNEL FILLED WITH FRESH WATER PRIOR TO THE TEST	Minimum Stream Nuclei (Tunnel Water Pressurized) Pr. (psia)	Time (hrs.)	Test Series	α (ppm)	Avg. Temp. °F
5/12/69	311	110	T2	75	24	-	-	-		50.5	22	A	5.30	74.3
6/12/69	312	95	T2	75	27 1/2	-	-	-		77.5	24	A	5.51	83.8
5/14/69	294	155	P1	75	24	-	-	-		56.0	21	A	5.44	78.6
5/21/69	295	105	P1	75	17	-	-	-		66.0	22	A	6.10	78.8
6/6/69	650	195	T01	75	16	-	-	-		61.5	22	A	5.05	77.0
6/16/69	560	85	T2	-	-	291	48	-		84.2	18	B	4.85	78.8
6/23/69	561	80	T2	-	-	1000	41	-		83.8	21 1/2	B	5.29	79.7
6/11/69	540	80	P1	-	-	700	24	-		83.0	20 1/2	B	5.35	81.9
6/17/69	541	85	P1	-	-	825	23	-		83.6	22 1/2	B	5.10	82.4
6/26/69	652	195	T01	-	-	1100	29	-		81.3	20	B	4.35	86.2
7/2/69	562	125	T2	-	-	1125	24	x		-	-	C	16.40	71.6
7/4/69	563	120	T2	-	-	1100	23 1/2	x		-	-	C	19.50	73.0
6/30/69	542	165	P1	-	-	1125	23	x		-	-	C	17.57	73.6
7/6/69	655	195	T01	-	-	1125	29	x		-	-	C	16.10	71.8
6/3/69	111	90	G1, α=5°	75	33	-	-	-		80.5	19	A	5.43	77.5
5/15/69	274	75	S1	75	24	-	-	-		56.0	24	A	5.00	79.2
5/22/69	275	90	S1	75	26	-	-	-		62.0	23	A	5.50	76.3
6/15/69	510	105	G1, α=5°	-	-	675	36	-		79.5	32	B	5.05	80.6
6/21/69	511	85	G1, α=5°	-	-	798	29	-		84.8	45	B	5.40	80.2
6/4/69	520	90	S1	-	-	214	22	-		77.0	21	B	5.53	75.4
6/8/69	521	80	S1	-	-	389	23	-		84.8	22	B	4.59	77.0
6/19/69	522	80	S1	-	-	842	28 1/2	-		84.5	48	B	5.05	78.8
6/29/69	512	460	G1, α=5°	-	-	1125	23 1/2	x		-	-	C	17.45	75.7
7/1/69	523	120	S1	-	-	1200	20 1/2	x		-	-	C	18.44	76.1
7/3/69	524	130	S1	-	-	1150	19 1/2	x		-	-	C	18.70	69.3
5/17/69	286	100	R1	75	24	-	-	-		53.0	21	A	5.95	78.3
5/28/69	287	90	R1	75	24	-	-	-		67.0	20	A	5.50	72.1
6/1/69	530	80	R1	-	-	251	24 1/2	-		68.7	21 1/2	B	5.30	82.4
6/10/69	531	85	R1	-	-	410	20	-		77.3	19 1/2	B	5.06	77.0
6/28/69	532	155	R1	-	-	1075	39	x		-	-	C	15.74	78.3
6/25/69	651	200	R01	75	22	-	-	-		81.0	21	A	4.91	82.9
6/27/69	653	185	R01	-	-	1125	26	-		82.3	24	B	4.85	88.3
7/5/69	654	195	R01	-	-	1125	30	x		-	-	C	16.10	74.3
5/18/69	307	90	T1	75	24	-	-	-		37.0	22	A	5.80	78.8
5/30/69	308	160	T1	75	24	-	-	-		56.3	21 1/2	A	4.95	82.6
6/7/69	309	130	T1	75	24	-	-	-		80.5	20 1/2	A	4.86	79.4
7/4/69	564	275	T1	75	25	-	-	x		-	-	-	19.20	74.4

TABLE 4
SUMMARY OF INCEPTION RUN DATA

P_s = 15.3 psia, $C_{P_{min}}$ = 0.69, $\bar{P}_v$ = 0.481 psia, V = 38.82 fps., $P_{min_i} = 1.69\ P_{\infty_i} - 15.3\ C_{P_{min}}$

1	2	3	4	5	6	7	8	9	10	11
Test No.	Test Series	Model	t_{i-1} (secs.)	t_{i-2} (secs.)	t_{i-av} (secs.)	t_{i-pav} (secs.)	$P_{\infty_{i-1}}$ (psia)	σ_{i-1}	$P_{min_{i-1}}$ (psia)	$\bar{\sigma}_d$
311, 312	A	T2	2.75	2.68	2.65	2.74	8.59	0.792	3.950	1.112
294,295	A	P1	3.04	3.31	3 32	5.03	8.04	0.738	3.030	0.973
560,561	B	T2	5.19	3.98	5.89	4.61	5.94	0.540	-0.530	0.948
540,541	B	P1	5.89	5.92	5.74	5.01	5.68	0.508	-0.990	0.785
562,563	C	T2	2.87	2.52	2.47	2.37	8.00	0.746	2.960	2.787
542	C	P1	2.87	2.30	2.49	2.98	7.95	0.741	2.860	2.600
111	A	G1,$\alpha'=5^o$	6.44	6.23	6.24	6.25	5.60	0.509	-	0.614
274,275	A	S1	6.28	6.59	6.41	6.43	5.64	0.512	-1.050	0.650
510,511	B	G1,$\alpha'=5^o$	5.52	5.40	5.87	6.67	5.82	0.533	-	0.604
520,521,522	B	S1	6.22	6.50	6.58	6.29	5.61	0.512	-1.100	0.654
512	C	G1,$\alpha'=5^o$	3.45	3.11	4.01	4.55	6.95	0.640	-	-
523,524	C	S1	4.13	3.22	3.08	4.43	6.60	0.608	0.560	-
286,287	A	R1	9.60	8.81	12.49	12.30	5.38	0.487	-1.510	0.687
530,531	B	R1	10.14	8.02	8.33	10.90	5.40	0.486	-1.460	0.652
532	C	R1	7.86	2.82	3.52	5.54	5.55	0.503	-1.200	1.352
650	A	T01	2.51	2.51	2.47	-	9.15	0.860	-	1.343
651	A	R01	2.74	3.31	4.76	-	8.60	0.803	-	1.335
652	B	T01	4.37	2.92	3.02	-	6.35	0.573	-	1.371
653	B	R01	5.59	2.74	2.72	-	5.75	0.509	-	1.338
655	C	T01	2.33	2.35	2.33	2.32	9.10	0.855	-	1.737
654	C	R01	2.47	2.40	2.42	2.65	8.78	0.819	-	1.519

TABLE 5

DATA FOR DESIVENT GASEOUS CAVITATION

Test No.	Model	Test Series	α (ppm)	V_{∞} (fps)	σ	Location of Spots of Cavitation at Desinence
295	P1	A	6.10	19.0	1.11n	Spots #3, 4 and 7 in Figure 14-b
295	P1	A	6.10	29.2	1.140	Spots #3, 4 and 7 in Figure 14-b
294*	P1	A	5.44	39.1	0.826	Simultaneous disappearance of many spots on both sides
542	P1	C	17.57	38.4	2.597	Spot #4 in Figure 14-b
308	T1	A	4.95	19.0	0.998	Spot #1 in Figure 15-b
308	T1	A	4.95	29.2	1.149	Spot #1 in Figure 15-b
309*	T1	A	4.80	38.9	1.097	Spots #2 and 9 in Figure 15-b
564	T1	-	14.20	39.0	2.707	Spot #2 in Figure 15-b
564	T1	-	19.20	29.2	4.363	Spots #2 and 7 in Figure 15-b
562*	T2	C	16.40	19.0	2.760	Spot #1 in Figure 16-b
563*	T2	C	19.50	39.0	2.814	Spot #3 in Figure 16-b

* Results of these tests are noted here in order to have a comparison of the values of desinent cavitation numbers for the corresponding models on different days. The repeatability of the cavitation number appears to be quite good. For the teflon model, at higher air contents, no repetition with the #1 model was carried out so that the results of the two tests with the #2 teflon nose have been listed and the comparison is again very good.

TABLE 6

DATA FOR INCIPIENT GASEOUS CAVITATION WITH TEFLON #1 NOSE AT A VELOCITY OF 39 FPS

Test No.	Run No	P_{sm_i} (psia)	P_{atm_i} (psia)	t_i (secs)	t_{cal} (secs)	t_d (secs)	Location of Cavitation Spots at Inception
306*	21	7.95	0.95	13.63	5.15	8.68	Spot #1, Figure 12-b
	22			60.00		54.85	Spot #6, Figure 12-b
	23			21.34		16.19	Spot #6, Figure 12-b
306	24	8.85	1.85	27.78	5.27	22.51	A flash near the location of spot #2, Figure 12-b
306	20	9.90	2.90	-	5.20	-	Waited for 300 seconds at 9.9 psia, but no cavitation was observed
309	10*	9.80	2.80	-	5.20	-	Waited for 600 seconds at 9.8 psia, but no cavitation was observed
	11*			275		270	Spot #4, Figure 12-b
	16**			-		-	Waited for 600 seconds at 9.8 psia, but no cavitation was observed
304**	27	17.80	10.80	2.82	3.61	-0.79	Spot #7, Figure 12-b
	28	17.70	10.70	1.22		-0.39	Spot #7, Figure 12-b
	31	16.15	11.15	1.24		-0.37	Many spots located near #2 and 3, Figure 12
	36	17.90	10.90	1.36		-0.05	Spots #2 and 8, Figure 12-b
304	18	19.05	12.05	4.63	3.54	1.09	Many spots around the nose
	29	18.90	11.90	1.78		0.24	Many spots near #2 and 3, Figure 12-b
	30	18.90	11.90	1.67		0.13	" " " " " " " "
	37	19.00	12.00	3.40		-0.14	" " " " " " " "
304	25	21.95	14.95	5.63	3.63	2.00	Many spots around the nose
	26	21.95	14.95	4.86		1.23	" " " " "
	32	21.90	14.90	4.49		0.86	Spot #2, Figure 12-b
	33	22.05	15.05	4.48		0.86	" " " "
304	20	25.55	18.55	15.00	3.30	11.70	Spot #7, Figure 12-b
	21	25.65	18.65	13.50		10.20	Same as in Run #20 and no other spot seen up to 260 seconds
	24	25.65	18.65	17.00		13.70	Spot #7, Figure 12-b. After 90 seconds spot #1 also appeared
	28	25.65	18.65	11.70		8.40	Spot #7, Figure 12-b
	34	26.15	19.15	11.64		8.34	" " " "
	35	26.05	19.05	10.29		6.99	" " " "

* An exposure pressure of 10.7 psia for 600 seconds was applied prior to the run.

** An exposure pressure of 60.6 psia for 300 seconds was applied prior to each run of this test.

* An exposure pressure of 16 psia for 300 seconds was applied prior to each run of this test.

** Tunnel was operated at a velocity of 39 fps for 300 seconds at a pressure of 5.5 psia. Then the flow was stopped and pressure set at 20 psia prior to the inception run.

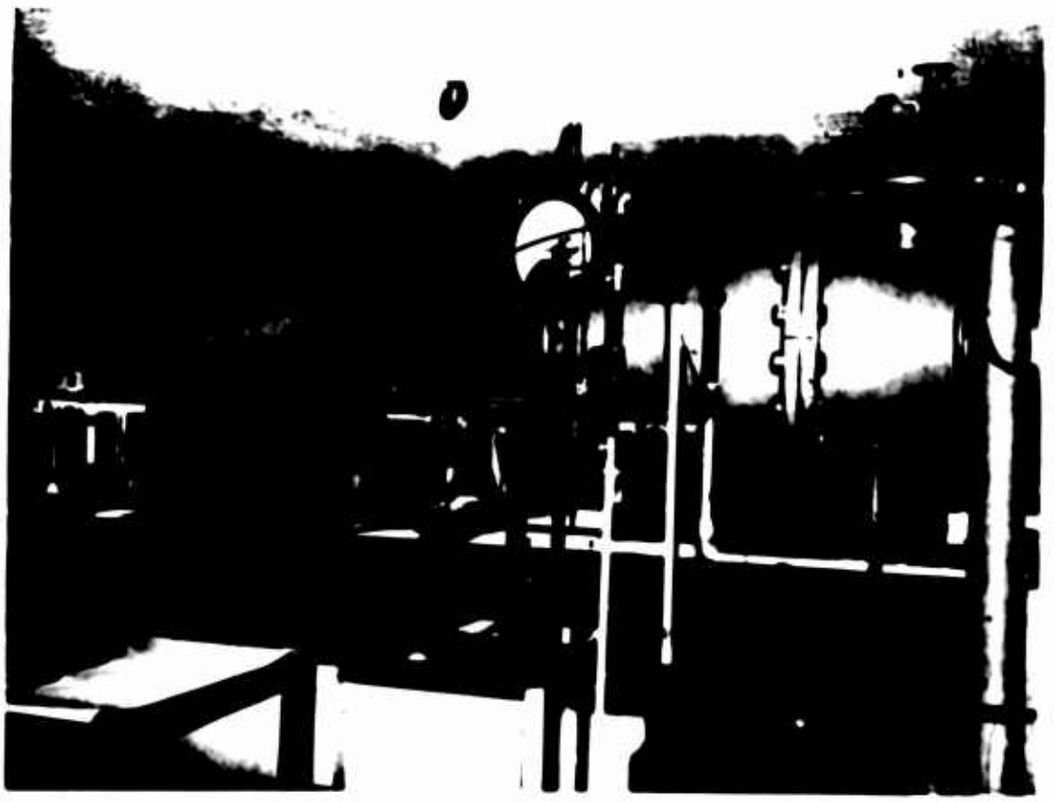

Figure 1. Photographic View of the Water Tunnel in the Region of the Test Section

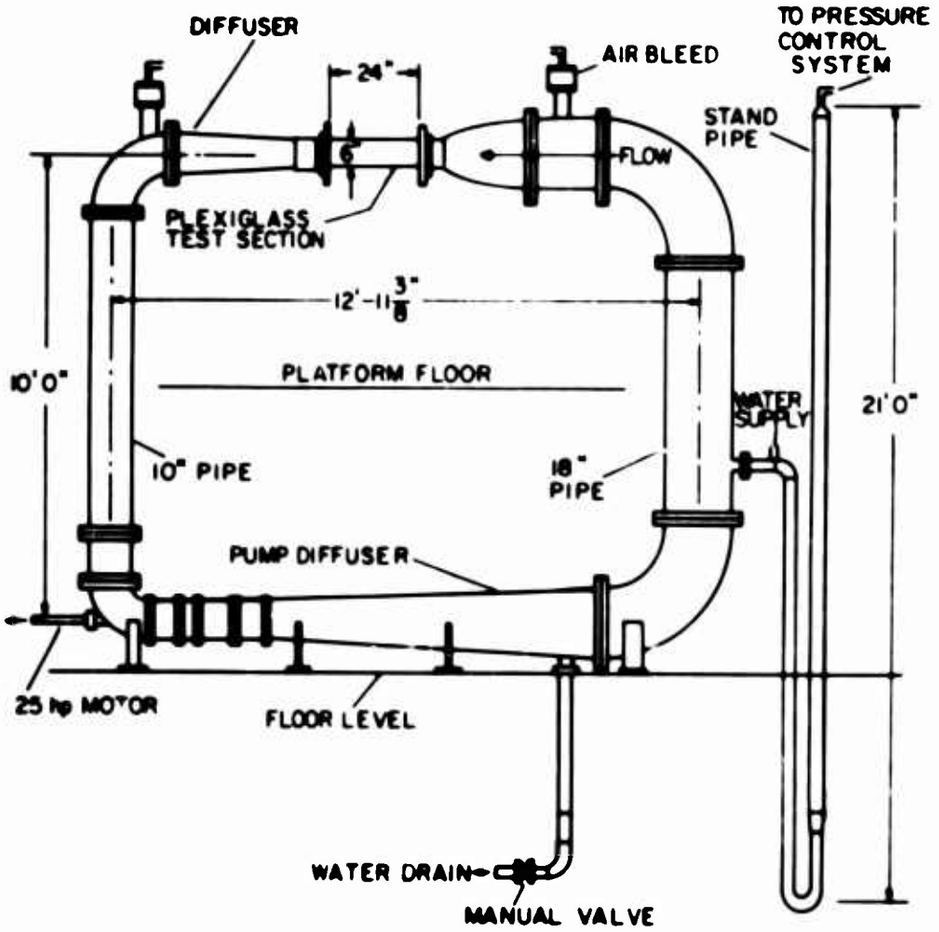

Figure 2. Diagram of the Tunnel Circuit

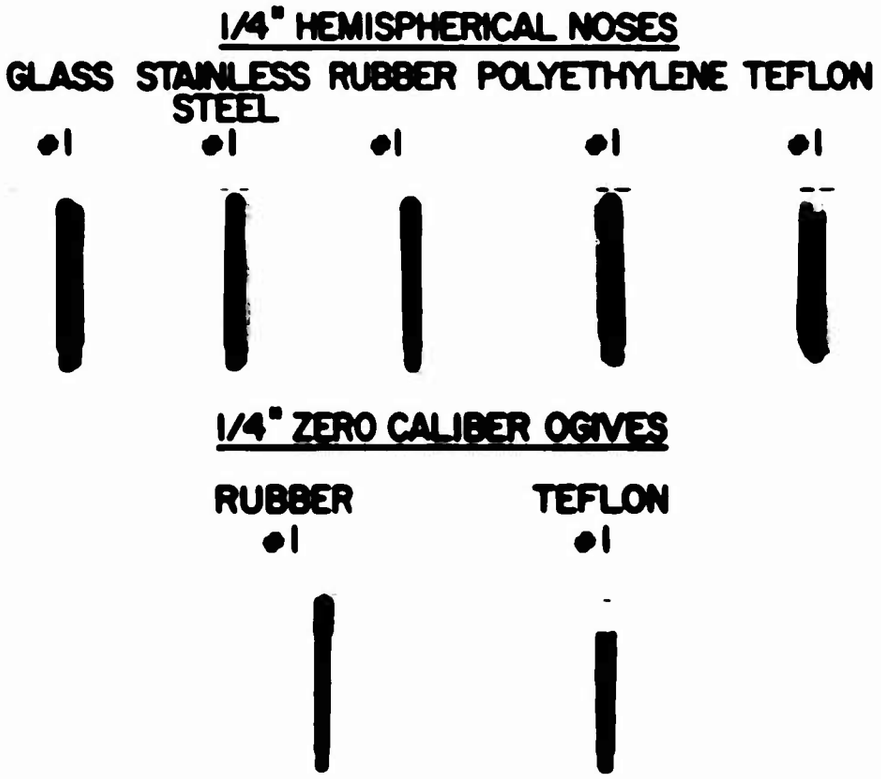

Figure 5. Photograph of the Test Models

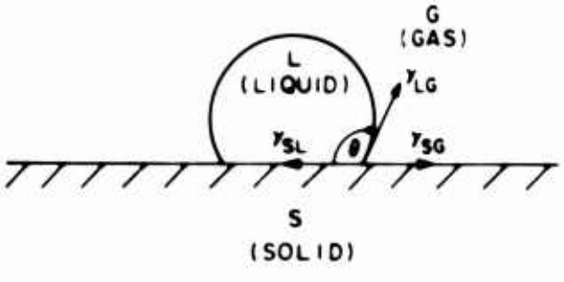

Figure 4. Equilibrium Contact Angle

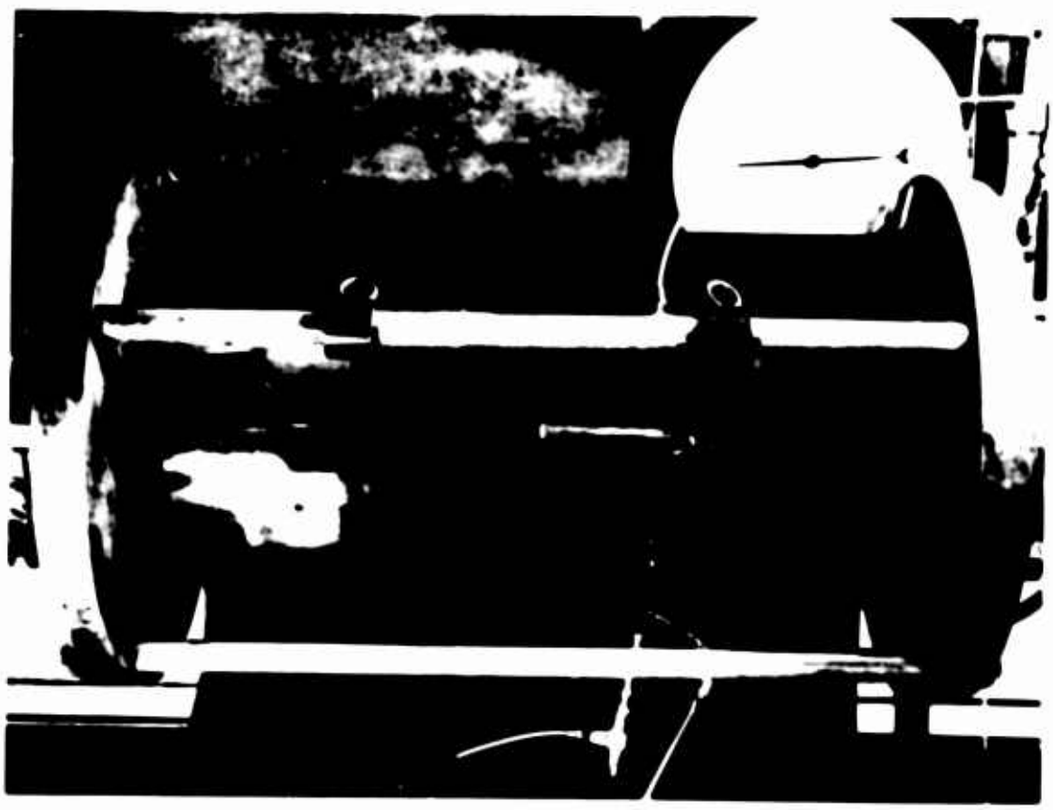

Figure 5. Test Model with Lucite Cap Mounted in the Test Section

Figure 6. Static Tank and Static Jacket

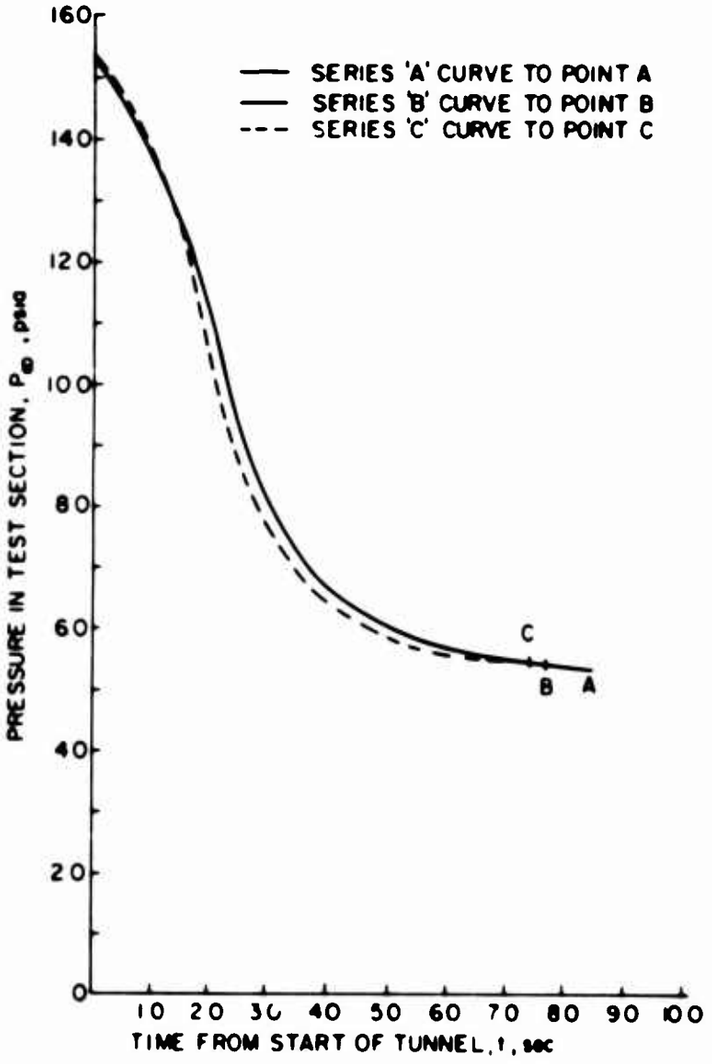

Figure 7. Gauge Response to Test Section Pressure During Tunnel Start-Up at High Speed

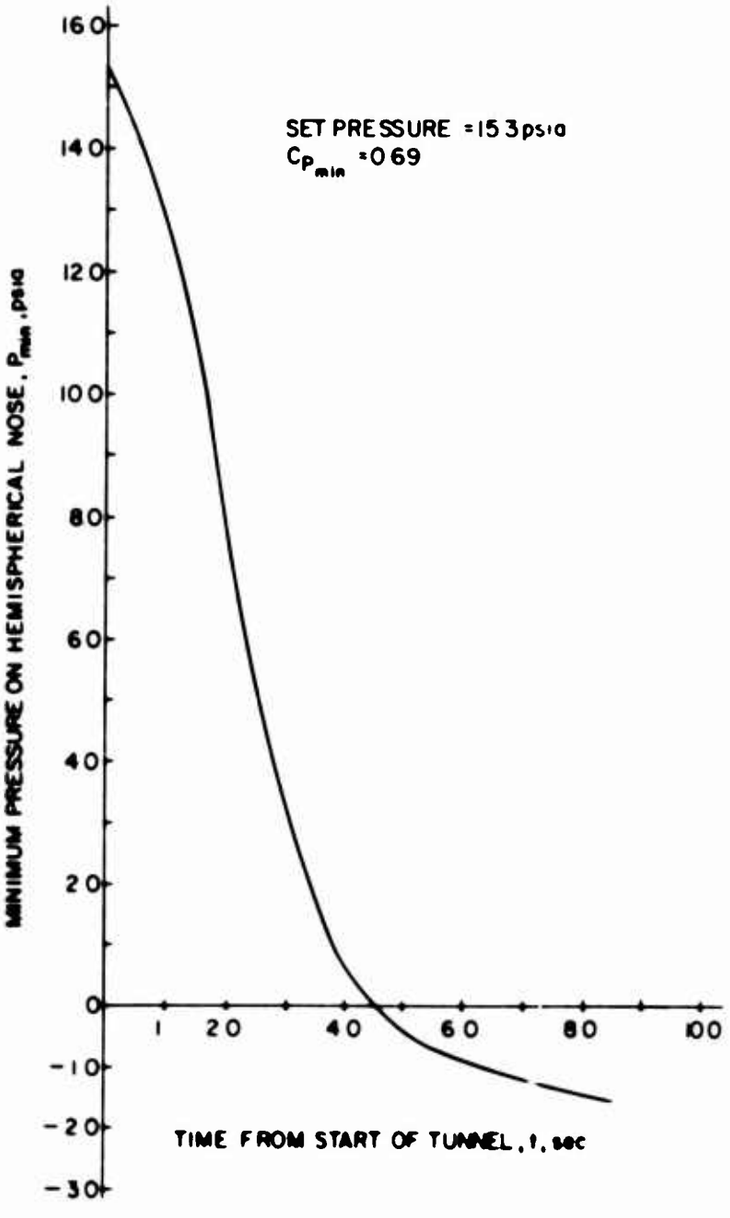

Figure 8. P_{min} Versus Time for a Hemispherical Nose During Tunnel Start-Up at High Speed

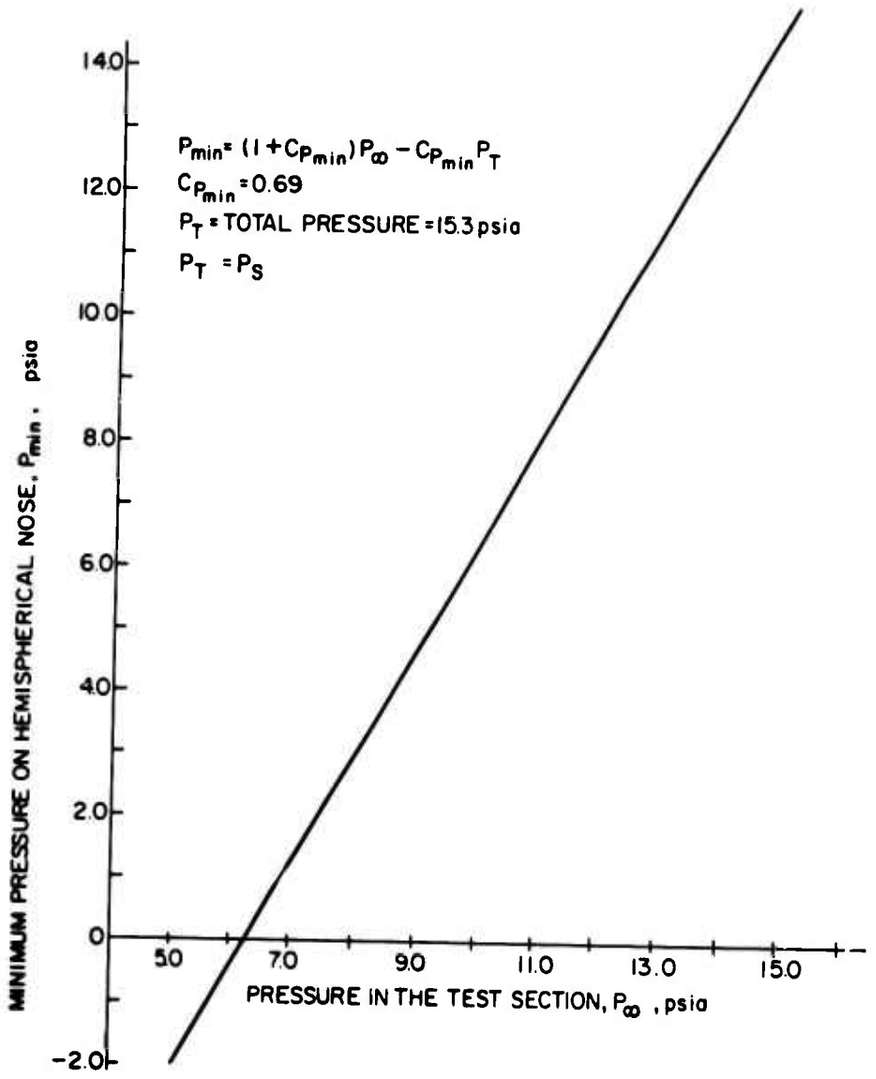

Figure 9. Test Section Pressure Versus Minimum Pressure on a Hemispherical Nose During Tunnel Start-Up at High Speed

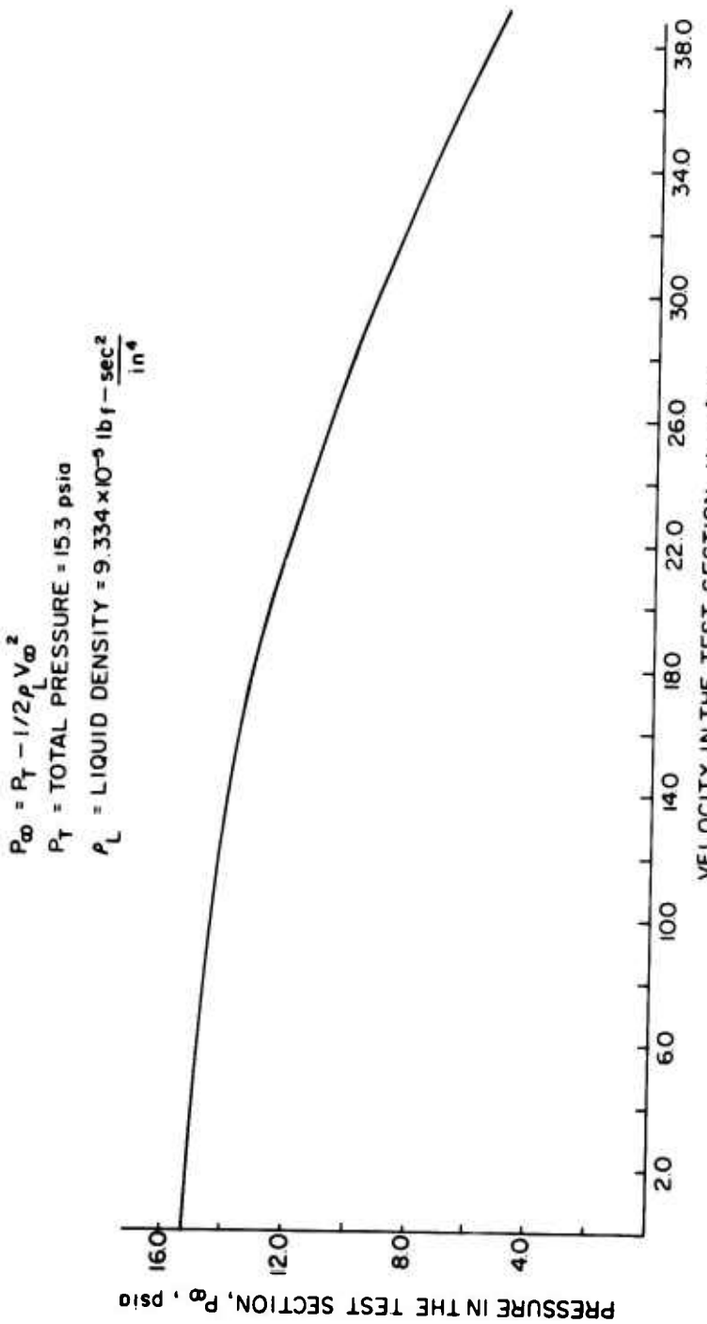

Figure 10. Pressure in the Test Section Versus Velocity During Tunnel Start-Up at High Speed

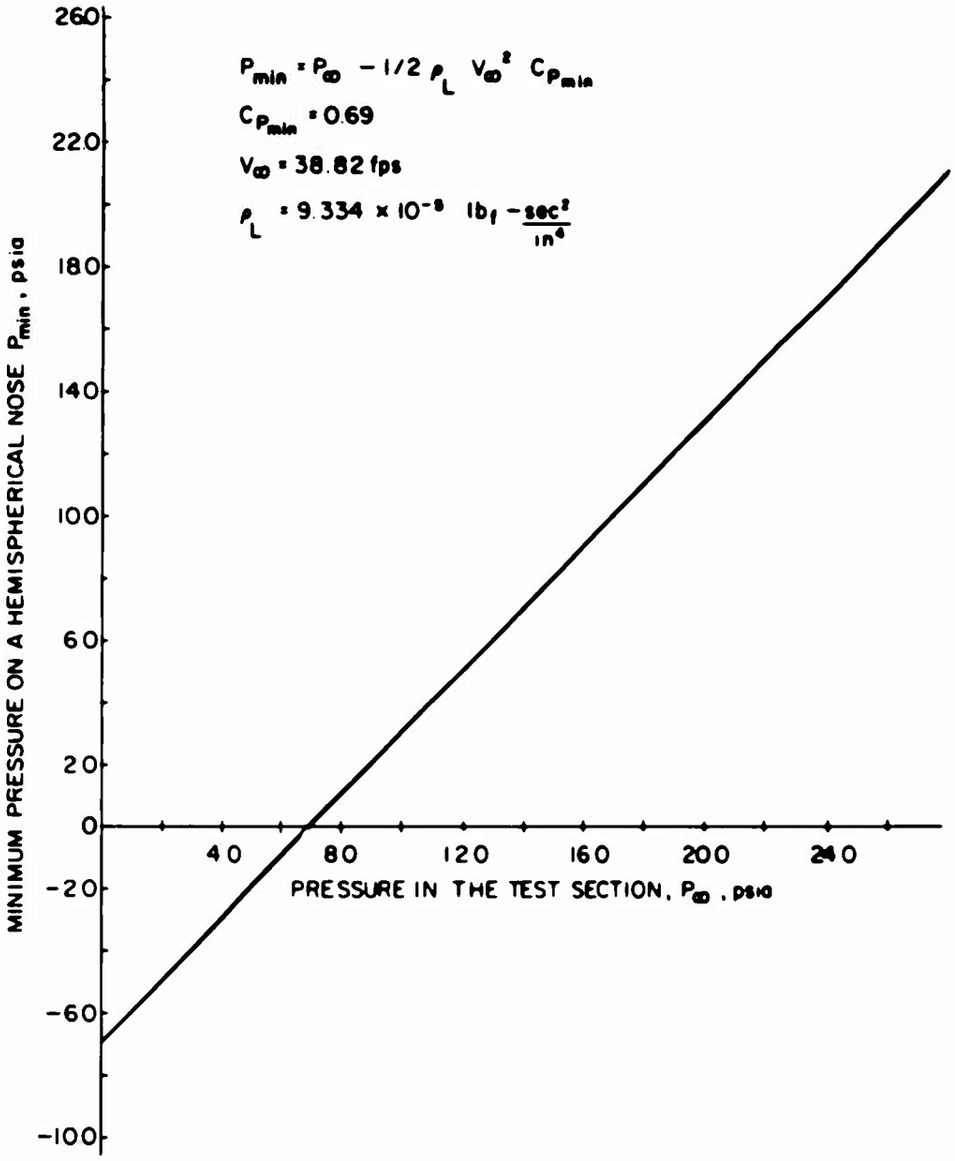

Figure 11. Test Section Pressure Versus Minimum Pressure on a Hemispherical Nose at Steady State

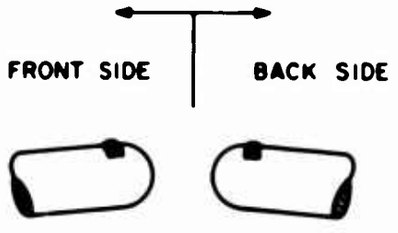

INCEPTION

(a)

DESINENCE
(FLASHING)

(b)

Figure 12. Cavitation on the 1/4" Glass Nose (G1) at $\alpha = 5^{\circ}$

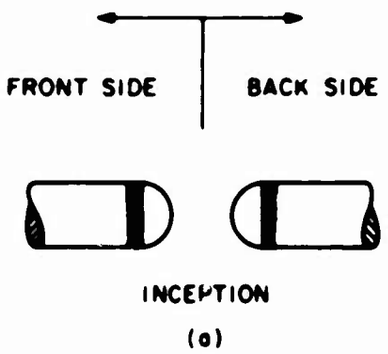

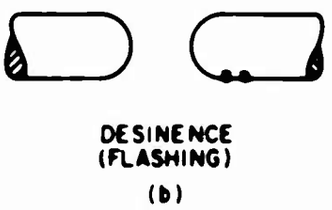

Figure 15. Cavitation on the 1/4" Stainless Steel Nose (S1)

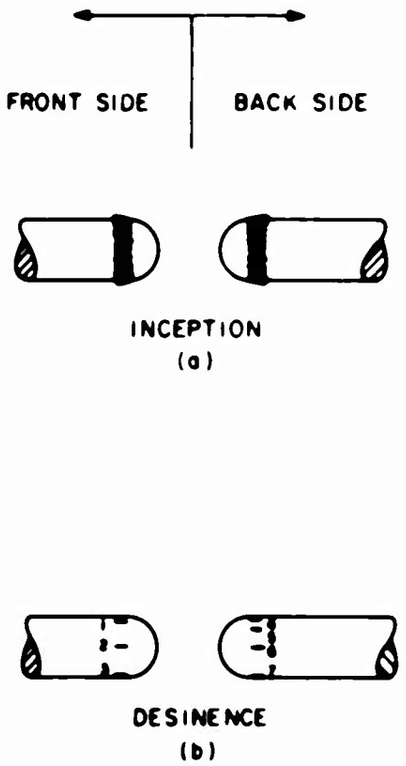

(ALL THE SPOTS OF CAVITATION DID NOT OCCUR IN A SINGLE RUN OR TEST)

Figure 14. Cavitation on the 1/4" Polyethylene Nose (P1)

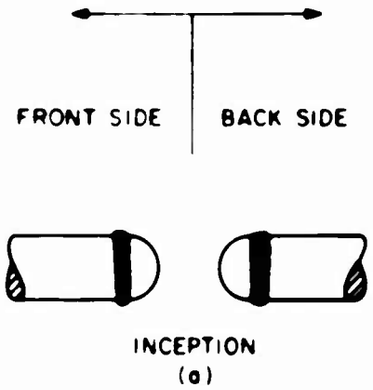

(ALL THE SPOTS OF CAVITATION DID NOT OCCUR IN A SINGLE RUN OR TEST)

Figure 15. Cavitation on the 1/4" Teflon #1 Nose (T1)

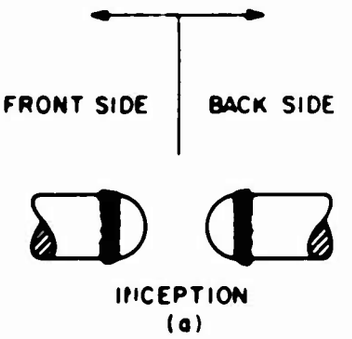

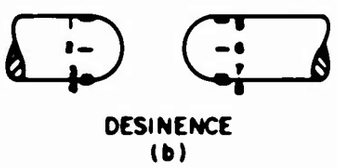

(ALL THE SPOTS OF CAVITATION DID NOT OCCUR IN A SINGLE RUN OR TEST)

Figure 16. Cavitation on the 1/4" Teflon #2 Nose (T2)

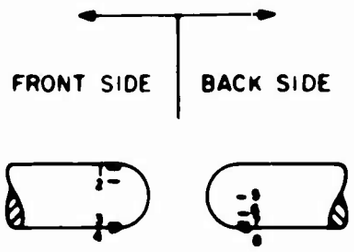

INCEPTION
(a)

(ALL THE SPOTS OF CAVITATION DID NOT OCCUR IN A SINGLE RUN OR TEST)

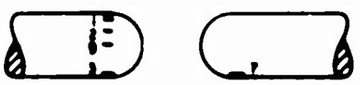

DESINENCE
(b)

(ALL THE SPOTS OF CAVITATION DID NOT OCCUR IN A SINGLE RUN OR TEST)

Figure 17. Cavitation on the 1/4" Rubber Nose (R1)

$$\sigma_d = C_p + \frac{\sigma_d \beta}{\frac{1}{2}\rho_L V_\infty^2} - \frac{2\gamma/r}{\frac{1}{2}\rho_L V_\infty^2} \qquad (52)$$

CURVES 1 & 5	CURVES 2 & 6
$C_p = 0.69$	$C_p = 0.877$
$\gamma = 4.14 \times 10^{-4}$ lb$_f$/in	$\gamma = 4.14 \times 10^{-4}$ lb$_f$/in
$r = 3.33 \times 10^{-4}$ in	$r = 2 \times 10^{-4}$ in
CURVES 3 & 7	**CURVES 4 & 8**
$C_p = 0.69$	$C_p = 0.877$
γ = ZERO	γ = ZERO

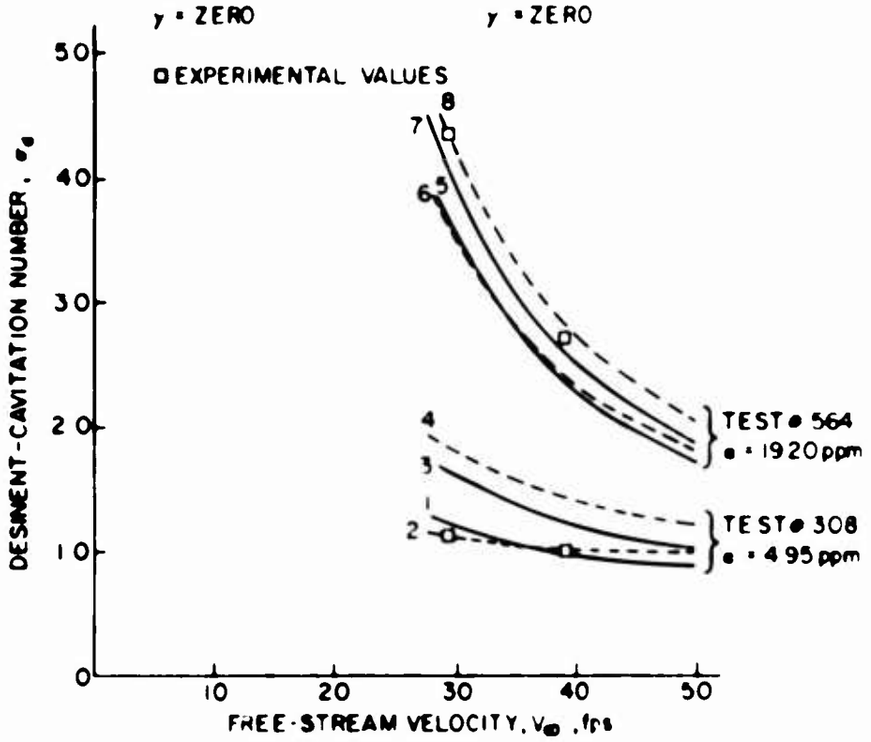

Figure 18. Desinent Cavitation Number Versus Free-Stream Velocity for the 1/4" Teflon Hemispherical Nose #1 (T1)

$$\sigma_d = C_p + \frac{\sigma_d \beta}{\frac{1}{2}\rho_L V_\infty^2} - \frac{2\gamma/r}{\frac{1}{2}\rho_L V_\infty^2} \quad \text{------(52)}$$

CURVES 1 & 5
$C_p = 0.69$
$\gamma = 4.14 \times 10^{-6} \frac{lb_f}{in}$
$r = 3.33 \times 10^{-6}$ in

CURVES 2 & 6
$C_p = 0.804$
$\gamma = 4.14 \times 10^{-6} \frac{lb_f}{in}$
$r = 2 \times 10^{-6}$ in

CURVES 3 & 7
$C_p = 0.69$
γ = ZERO

CURVES 4 & 8
$C_p = 0.804$
γ = ZERO

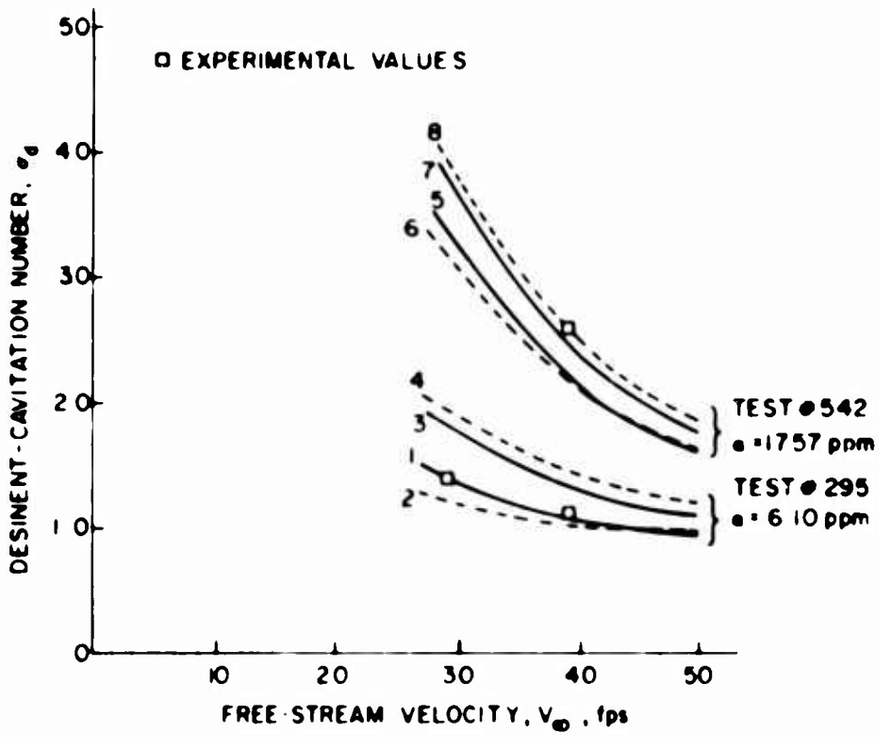

Figure 19. Desinent Cavitation Number Versus Free-Stream Velocity for the 1/4" Polyethylene Hemispherical Nose #1 (P1)

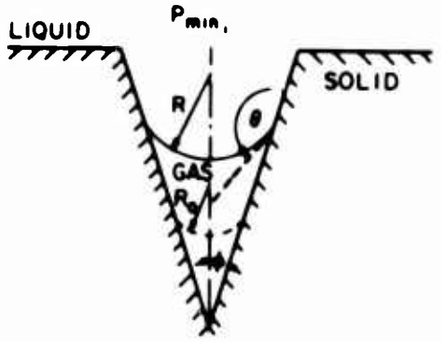

$$\epsilon = \frac{R}{R_o}$$

$$P_L = P_{min.} = P_V + P_G + \frac{2\gamma}{R}$$

Figure 20. Idealized Surface Nucleus for Incipient Gaseous Cavitation

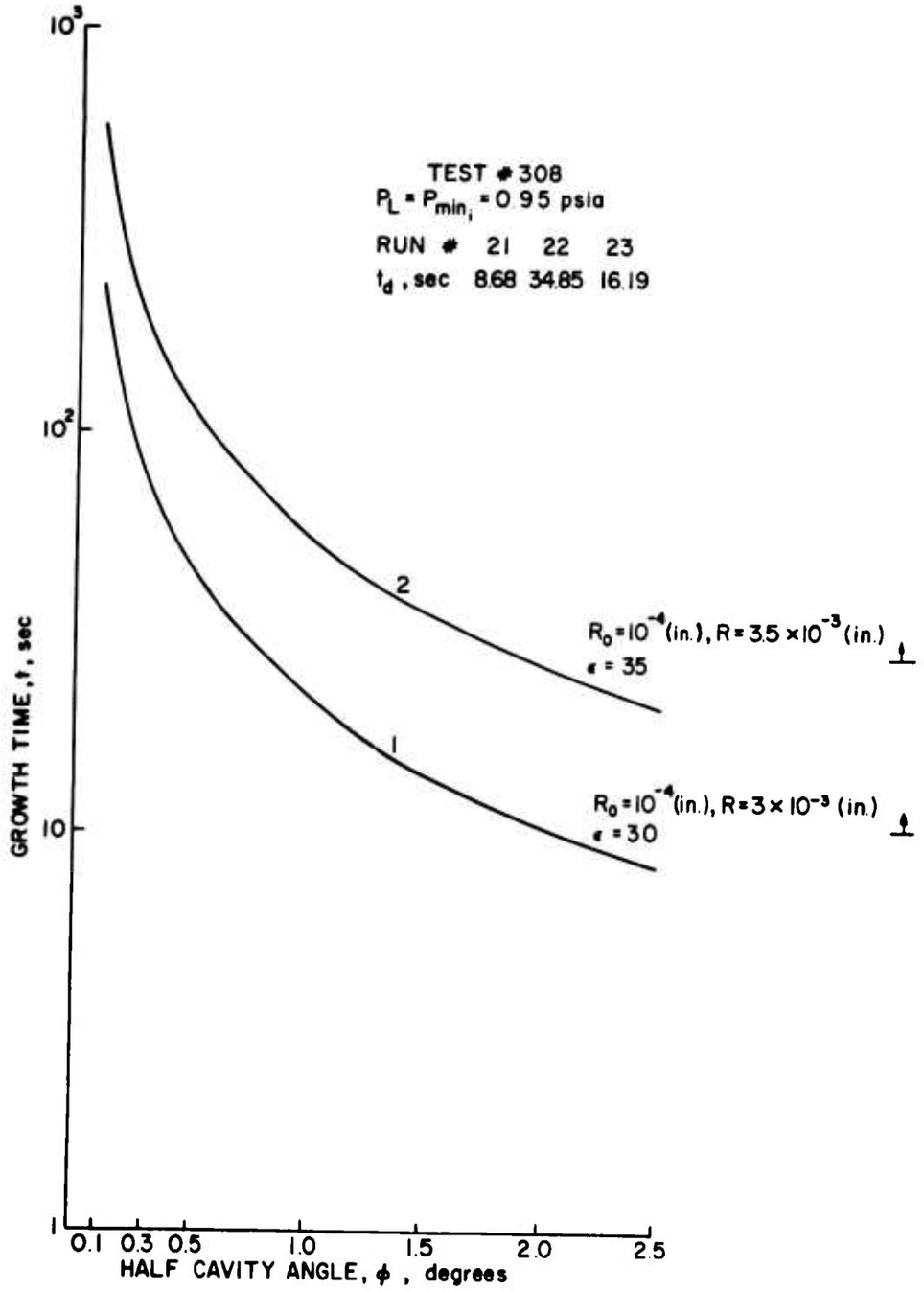

Figure 21. Growth Time Versus Half Cavity Angle

DOCUMENT CONTROL DATA - R & D

(Security classification of title, abstract and indexing annotation when overall report is classified)

1. ORIGINATING ACTIVITY (Corporate author) Ordnance Research Laboratory University Park, Pennsylvania	2a. REPORT SECURITY CLASSIFICATION UNCLASSIFIED 2b. GROUP ---

3. REPORT TITLE

THE INFLUENCE OF POROSITY AND CONTACT ANGLE ON INCIPIENT AND DESINENT CAVITATION

4. DESCRIPTIVE NOTES (Type of report and inclusive dates)

Thesis, December 15, 1969

5. AUTHOR(S) (First name, middle initial, last name)

S. K. Gupta

6. REPORT DATE December 15, 1969	7a. TOTAL NO. OF PAGES 90 pp.and figs.	7b. NO. OF REFS 20
8a. CONTRACT OR GRANT NO. NOw 65-0123-d b. PROJECT NO. c. d.	9a. ORIGINATOR'S REPORT NUMBER(S) TM 508.2451-06 9b. OTHER REPORT NO(S) (Any other numbers that may be assigned this report) None	

10. DISTRIBUTION STATEMENT

Distribution of this document is unlimited

11. SUPPLEMENTARY NOTES None	12. SPONSORING MILITARY ACTIVITY Naval Ordnance Systems Command Department of the Navy

13. ABSTRACT

This investigation was primarily devoted to the determination of the effect of porosity and contact angle on incipient and desinent cavitation. The primary test models were 1/4-inch diameter hemispherical-nosed bodies made of teflon, rubber, polyethylene, stainless steel and glass. The test results imply that the hydrophobic surfaces, i.e., teflon and polyethylene models contribute surface nuclei to the inception process provided that the surface nuclei are in a normal condition, i.e., no effort has been made to minimize surface nuclei by extreme pressurization, etc. On the other hand, the hydrophilic hemispherical models made of glass and stainless steel seem to show no contribution of surface nuclei to the onset of cavitation and may depend entirely on the stream nuclei for cavitation. However, the rubber model which was hydrophilic in nature was not consistent with the other hydrophilic models.

DD FORM 1 NOV 65 1473

14. KEY WORDS	LINK A		LINK B		LINK C	
	ROLE	WT	ROLE	WT	ROLE	WT
Cavitation number	8					
Desinent cavitation	8					
Gaseous cavitation	8					
Glass	8					
Goniometer	8					
Helium-mercury	8					
Hemispherical nose	8					
Incipient cavitation	8					
Lucite cap	8					
Ogive nose	8					
Polyethylene	8					
Porosity	8					
Pressure response	8					
Pseudo-cavitation	8					
Rubber	8					
Stainless steel	8					
Surface nuclei	8					
Teflon	8					
Vaporous cavitation	8					
Zero caliber	8					